MOLECULAR AND CELLULAR BIOLOGY, Feb. 2010, p. 657–674 Vol. 30, No. 3
0270-7306/10/$12.00 doi:10.1128/MCB.01117-09

Fission Yeast Iec1-Ino80-Mediated Nucleosome Eviction Regulates Nucleotide and Phosphate Metabolism▽

Cassandra Justine Hogan,[1] Sofia Aligianni,[1]† Mickaël Durand-Dubief,[1] Jenna Persson,[2] William R. Will,[1] Judith Webster,[4] Linda Wheeler,[3] Christopher K. Mathews,[3] Sarah Elderkin,[1] David Oxley,[4] Karl Ekwall,[2] and Patrick Daniel Varga-Weisz[1]*

Chromatin and Gene Expression, Babraham Institute, Babraham, Cambridge CB22 3AT, United Kingdom[1]; Karolinska Institutet, Department of Biosciences and Nutrition, and University College Södertörn, Novum S-141 57 Huddinge, Sweden[2]; Department of Biochemistry and Biophysics, Oregon State University, Corvallis, Oregon[3]; and Proteomics Group, Babraham Institute, Babraham, Cambridge CB22 3AT, United Kingdom[4]

Received 18 August 2009/Returned for modification 21 October 2009/Accepted 16 November 2009

Ino80 is an ATP-dependent nucleosome-remodeling enzyme involved in transcription, replication, and the DNA damage response. Here, we characterize the fission yeast Ino80 and find that it is essential for cell viability. We show that the Ino80 complex from fission yeast mediates ATP-dependent nucleosome remodeling *in vitro*. The purification of the Ino80-associated complex identified a highly conserved complex and the presence of a novel zinc finger protein with similarities to the mammalian transcriptional regulator Yin Yang 1 (YY1) and other members of the GLI-Krüppel family of proteins. Deletion of this Iec1 protein or the Ino80 complex subunit *arp8*, *ies6*, or *ies2* causes defects in DNA damage repair, the response to replication stress, and nucleotide metabolism. We show that Iec1 is important for the correct expression of genes involved in nucleotide metabolism, including the ribonucleotide reductase subunit *cdc22* and phosphate- and adenine-responsive genes. We find that Ino80 is recruited to a large number of promoter regions on phosphate starvation, including those of phosphate- and adenine-responsive genes that depend on Iec1 for correct expression. Iec1 is required for the binding of Ino80 to target genes and subsequent histone loss at the promoter and throughout the body of these genes on phosphate starvation. This suggests that the Iec1-Ino80 complex promotes transcription through nucleosome eviction.

The structure of chromatin is modulated by chromatin-remodeling factors, such as histone-modifying enzymes and ATP-dependent chromatin-remodeling complexes (7, 35, 45, 54). The latter are usually multisubunit protein complexes containing an ATPase from the SWI2/SNF2 superfamily, which uses the energy derived from ATP hydrolysis to disrupt histone-DNA interactions (6, 13, 26).

Ino80 is a member of this SWI2/SNF superfamily and is the catalytic subunit of the Ino80 chromatin-remodeling complex (65). Initially characterized in budding yeast (*Saccharomyces cerevisiae*), the Ino80 complex plays a central role in DNA-mediated processes, such as DNA double-strand break repair, homologous recombination, and the regulation of the DNA damage cell cycle checkpoint response, chromosomal-DNA replication, and transcription (5, 10, 18, 23, 24, 38, 39, 52, 56, 57, 65, 69, 74, 76, 80, 82; reviewed in reference 4). Ino80 complexes purified from budding yeast and mammalian cells contain core subunits, which are conserved across species, as well as species-specific proteins (36, 65). In budding yeast, the core Ino80 complex is composed of INO80, ARP5, ARP8, ARP4, RVB1, RVB2, IES2, and IES6 (63, 65). The actin-like proteins ARP5 and ARP8 are unique to the Ino80 complex and are required for an active complex in budding yeast (38, 63). ARP4 plays a role in the response to DNA damage in budding yeast and is also a member of the chromatin-remodeling complex SWR1 and the histone acetyltransferase complex NuA4 (16, 42, 52, 76). The Rvb1 and Rvb2 proteins (also called Pontin/Tip49 and Reptin/Tip48, respectively, in mammalian cells) are AAA^+ ATPases related to the Holliday junction-resolving RUVB proteins of bacteria (65). They are integral members of the Ino80- and SWR1-remodeling complexes (36, 42, 43, 50, 65), as well as the histone acetylase Tip60 complex (34) and the transcription activator c-Myc complex (reviewed in references 25 and 81). Ies2 and Ies6 are conserved from yeast to humans and have direct roles in transcriptional regulation in mammalian cells (10, 63).

A YY1-containing Ino80 complex was recently identified in mammalian and *Drosophila* cells (10, 41, 82). Yin yang-1 (YY1) is a zinc finger-containing Polycomb group (PcG) transcription factor that regulates genes essential for growth and development (1, 9, 15, 68). The mammalian YY1-Ino80 complex has been found to play roles in transcription and homologous-recombination-based repair (10, 82).

The precise mechanisms by which Ino80 regulates cellular processes are unclear. Unlike budding yeast, which has very little higher-order chromatin, the fission yeast (*Schizosaccharomyces pombe*) offers a more complex chromatin structure that is more similar to that of higher eukaryotes in many respects (for a review, see reference 28). Therefore, the char-

* Corresponding author. Mailing address: Chromatin and Gene Expression, Babraham Institute, Babraham, Cambridge CB22 3AT, United Kingdom. Phone: 44 (0) 1223 496434. Fax: 44 (0) 1223 496022. E-mail: Patrick.varga-weisz@bbsrc.ac.uk.

† Present address: Division of Biological Sciences, University of California San Diego, La Jolla, CA.

▽ Published ahead of print on 23 November 2009.

TABLE 1. *S. pombe* strains used in this study

Strain	Genotype	Source
JZ1	h^{90} *ade6-210 leu1-32 ura4-D18*	J. Dalgaard
JZ5	*matM smt-0 ade6-M216 leu1-32*	J. Dalgaard
FY367	h^+ *ade6-210 leu1-32 ura4-D18*	R. Allshire
FY2317	h^+ *leu1-32*::nENT1-*leu1*$^+$ (pJAH29)*his7-366*::*hsv-tk-his7*$^+$ (pJAH31)*ura4-D18 ade6-210*	S. Forsburg
SA001	FY2317 *ino80* V5Flag/Kan^r	This study
CH001	JZ1 *ura4-D18* Δ*iec1*::*ura4*$^+$	This study
CH003	SA001 *ura4-D18* Δ*iec1*::*ura4*$^+$	This study
CH004	JZ1 *ura4-D18 iec1* HA::*ura4*$^+$	This study
CH006	SA001 *ura4-D18 iec1* HA::*ura4*$^+$	This study
CH007	CH001+pIec1 (pNMT81-*iec1 leu*$^+$)	This study
CH008	JZ1+pSA01 (empty pNMT81 vector *leu*$^+$)	This study
CH009	CH001+pSA01 (empty pNMT81 vector *leu*$^+$)	This study
CH010	FY367 Δ*nhp10*/Kan^r	This study
CH011	FY367 Δ*arp8*/Kan^r	This study
CH012	JZ1 Δ*ies2*/Kan^r	This study
CH013	FY367 Δ*ies6*/Kan^r	This study
CH014	CH001 Δ*ies2*/Kan^r	This study
CH015	FY367 *ura4-D18* Δ*iec1*::*ura4*$^+$	This study
CH016	SA001 *iec1* MYC/Nat^r	This study
SA002	FY367 + pSA01 (empty pNMT81 vector *leu*$^+$)	This study
SA003	*leu1-32* Δ*ino80*/Kan^r + pSA02 (pNMT81-*ino80 leu*$^+$)	This study

TABLE 2. Primer pairs for the deletion of Ino80 complex subunits *iec1*, *nhp10*, *arp8*, *ies6*, and *ies2*

Gene	Sequence
5′ upstream region	
iec1	5′-GAGACGGCCGGTCGAACCAATTCAGTTCAGC-3′
	5′-GAGAGAATCCGAACCTCAACAACTCACAAGTG-3′
nhp10	5′-GAGACGGCCGGTTGAGTCGATTTCTAAGGAGG-3′
	5′-GAGAGGATCCATAGATGCTCTGCCTTTGAT-3′
arp8	5′-GAGACGGCCGCCTACACACGCACATCCT-3′
	5′-GAGAGGATCCTGGTCATCCCTTTTGAC-3′
ies6	5′-GAGACGGCCGGCCGAAGAGGTGAAGCTAGCTA-3′
	5′-GAGAGGATCCGCCGCACTTCTTCTATGTATCG-3′
ies2	5′-GAGACGGCCGTGCAAATCAACGGTCGAC-3′
	5′-GAGAGGATCCCAGAAGCTGCTAAGTTTCACAG-3′
3′ downstream region	
iec1	5′-GAGACTCGAGGATGCATCTTCAAATGCCTTACG-3′
	5′-GAGAGGTACCGATACAACCACACTAAGGCAG-3′
nhp10	5′-GAGAGAATTCAGCTTTCTGATGCAGGC-3′
	5′-GAGAAAGCTTCAATCATTCGTCGTTACCACG-3′
arp8	5′-GAGAGAATTCCAGTACAGATGCCTCTAAG-3′
	5′-GAGAAAGCTTGCAATGCTGAGTCTCTCAAG-3′
ies6	5′-GAGAGAATTCGAAGTGCATTAGACCAGGTATG-3′
	5′-GAGAAAGCTTCAGCTTACGGATGCTTGTCTAC-3′
ies2	5′-GAGAGAATTCGTAATAACACTTCGCATATTCGC-3′
	5′-GAGAAAGCTTTCCATACATCAGGACGGCT-3′

acterization of the Ino80 complex in this model organism may give new insights into the functions and mechanisms of this versatile complex.

Here, we characterize the fission yeast Ino80 complex. The purified complex mediated ATP-dependent nucleosome remodeling *in vitro*. We found that the complex is highly conserved through evolution and contains a novel factor, Iec1 (67). Iec1 bears sequence similarity to YY1 and other members of the GLI-Krüppel family of zinc finger proteins. Iec1 and the Ino80 complex subunits *arp8*, *ies6*, and *ies2* are important for efficient DNA damage repair and the response to replication stress. The double deletion of *iec1* and *ies2* suppresses defects of the single deletions, suggesting that the different Ino80-interacting proteins may program the complex in different, possibly opposing ways. We show that Iec1 is important for the regulation of several genes involved in nucleotide and phosphate metabolism. Iec1 is required for the binding of Ino80 to the promoter and downstream regions of these genes, leading to reduced nucleosome density over the locus. We suggest that the Iec1-Ino80 complex regulates the transcription of genes involved in nucleotide metabolism by mediating nucleosome eviction.

MATERIALS AND METHODS

Yeast strains and media. The *S. pombe* strains used in this study are listed in Table 1. Cells were grown in rich yeast extract with supplements (YES) or Edinburgh minimal medium (EMM) at 30°C unless otherwise indicated (51). Histidine, leucine, uracil, and lysine were added at 250 mg/liter and adenine at 250 mg/liter, or 2 mg/liter for low-adenine media. Low-phosphate EMM was prepared by replacing potassium hydrogen phthalate and Na_2HPO_4 with NaH_2PO_4 (10 mg/liter) and NaOAc (1 g/liter). Inorganic phosphate was removed from YES by precipitation as magnesium phosphate under alkaline conditions (62). Hydroxyurea (HU) (Sigma) was added to the medium at 7.5 mM and bleocin (Calbiochem) at 3 μg/ml. For UV irradiation, the plates were placed in a Stratalinker UV cross-linker and exposed to 100 J/m^2.

Construction of a FLAG-tagged Ino80-expressing strain. The SA001 strain expressing Ino80 with C-terminal FLAG tags from the endogenous locus was generated using strain FY2317. A plasmid was constructed that drove expression of FLAG- and V5-tagged *S. pombe* Ino80 from the NMT81 promoter, using the pNMT81-TOPO system (Invitrogen). In this plasmid the *ino80* cDNA was followed by a kanamycin resistance cassette, followed by a 174-bp fragment of sequence just 3′ to the *ino80* open reading frame (ORF). The replacement cassette was amplified from this construct with *Pfu* Ultra (Stratagene) with primers 5′-ACTTTCAACAAGGGCAGGTGGTTTGGG-3′ and 5′-GTCGAC TGTTTACAACATTTCATCTAA-3′. The FLAG-tagged protein has a modified flag tag at the C terminus (only one D), followed by a 6-amino-acid spacer, then by the V5 tag, then by a 5-amino-acid spacer, and by a double FLAG tag.

Construction of *iec1* deletion strains. The entire *iec1* ORF was deleted by homologous recombination (29). The URA4 gene was ligated into the HindIII site of pBluescript, giving rise to pURA. PCR products representing the 5′ upstream region of the *iec1* ORF were prepared with the upstream primers (Table 2) and digested with EcoRI and EagI. The 3′ downstream region of the *iec1* ORF was prepared with primers listed in Table 2 and digested with XhoI and KpnI. Both PCR fragments were inserted on either side of the URA4 gene in pURA. This URA4 deletion cassette was amplified by PCR and transformed into cells by the lithium acetate procedure (19). Colonies were selected for growth in medium lacking uracil. Positives were verified by PCR using primer pairs outside the cassette.

Construction of hemagglutinin (HA)-tagged Iec1-expressing strains. A PCR fragment representing the *iec1* ORF and incorporating a C-terminal HA tag was prepared with the primers 5′-GAGACGGCCGCATGTCTATATCCTCGGAT ACCTC-3′ and 5′-GAGAGAATTCCGCATAATCCGGCACATCATACGGA TAACGACTGATGCTGGGATCCACTT-3′, digested with EagI and EcoRI, and, along with the 3′ downstream region of *iec1* digested with XhoI and KpnI, inserted on either side of the URA4 gene in pURA as described above. The cassette was then amplified by PCR and transformed into yeast. Positive clones were selected for growth on medium lacking uracil and were verified for correct integration by PCR and by Western blot analysis of whole-cell extracts using anti-HA antibody (Roche).

Construction of 13MYC-tagged Iec1-expressing strains. PCR products representing the *iec1* ORF prepared with the primers 5′-GAGAGAGTCGACGGA TGTCTATATCCTCGGATACCTCA-3′ and 5′-TCTCTCTTAATTAAACGA CTGATGCTGGGATCCACTTG-3′ digested with SalI and PacI and the 3′downstream region of the *iec1* ORF prepared with the primers 5′-GAGAGA GAGCTCGATGCATCTTCAAATGCCTTACG-3′ and 5′-TCTCTCATCGAT GATACAACCACACTAAGGCAG-3′ digested with SacI and ClaI were inserted on either side of the 13MYC-natMX6 cassette in the pFA6a-13Myc-natMX6 plasmid (78). The resulting cassette was amplified by PCR and transformed into yeast using the lithium acetate procedure (19). Positive clones were selected for growth on medium containing 100 μg/ml nourseothricin (ClonNAT; Werner Bioagents) and were validated by PCR and by Western blot analysis of whole-cell extracts using anti-Myc antibody (Cell Signaling).

Construction of *nhp10*, *arp8*, *ies6*, *ies2*, and *ino80* deletion strains. The kanMX6 cassette was cleaved out of the pFA6a-kanMX6 plasmid by digestion with EcoRI and BamHI and ligated into EcoRI/BamHI-cleaved pBluescript, giving rise to pKAN (3, 32, 78). The 5′ upstream region and 3′ downstream

regions of the *nhp10*, *arp8*, *ies6*, and *ies2* ORFs were amplified with the primers listed in Table 2 and digested with EagI and BamHI for the 5′ fragment and EcoRI and HindIII for the 3′ fragment. The 5′ and 3′ fragments were inserted on either side of the kanx cassette in pKAN. This kanx deletion cassette was amplified by PCR, and *nhp10*, *arp8*, *ies6*, and *ies2* were deleted by homologous recombination (29). Positive clones were selected for growth in YES medium supplemented with 150 mg/liter G418 (Invitrogen) and verified by PCR using one primer upstream of the cassette and one within the kanx cassette. *ino80* was deleted by replacing the entire ORF with the kanx cassette in a diploid strain that was generated by mating JZ1 with JZ5.

Purification of the FLAG-tagged Ino80 complex and the MYC- or HA-tagged Iec1 complexes from *S. pombe*. The protocol for the purification of the FLAG-tagged Ino80 complex and the MYC- or HA-tagged Iec1 complexes from *S. pombe* was adapted from the method of Tsukiyama et al. (73). Briefly, cultures of the SA001, FY2317 (as a control), CH006, and CH004 strains were grown to saturation in EMM. The cells were pelleted and washed once with ice-cold water, once with H buffer (25 mM HEPES, pH 7.6, 0.5 mM EGTA, 0.1 mM EDTA, 2 mM $MgCl_2$, 20% glycerol, 0.02% NP-40, 1 mM dithiothreitol [DTT])-300 mM KCl and once with H buffer-300 mM KCl supplemented with Complete EDTA-free protease inhibitor cocktail (Roche). The cells were then frozen in liquid nitrogen and broken in dry ice using a coffee mill. The cells were resuspended in H buffer-500 mM KCl with Complete EDTA-free protease inhibitor (Roche) and spun at 37 K in a SW40 Beckman rotor. The supernatant (~20 ml) was recovered and incubated on a rotating wheel with 100 μl FLAG-M2 agarose beads (Sigma) or 100 μl anti-HA (Roche) monoclonal antibodies coupled to protein A for 3 h at 4°C. The beads were washed 5 times with H buffer-500 mM KCl and twice with H buffer-150 mM KCl. The Ino80 complex was then eluted from the beads by incubating them 4 times with 100 μl 2.5-mg/ml FLAG-peptide (Sigma) in 12.5 mM HEPES, pH 7.6, 7.5 mM Tris, pH 7.4, 75 mM KCl, 75 mM NaCl, 0.5 mM EGTA, 0.1 mM EDTA, 2 mM $MgCl_2$, 20% glycerol, 0.02% NP-40, 1 mM DTT, and Complete EDTA-free protease inhibitor (Roche). For the immunoprecipitation of the HA-tagged complexes, strains CH006 and SA001 (as a control) were used. For mass spectrometric analysis, beads were washed with 25 mM ammonium bicarbonate and proteins were eluted with 6 M guanidine hydrochloride. The amount of protein was determined by SDS-PAGE following Coomassie blue staining by comparing the band intensity with those from a bovine serum albumin standard.

For the immunoprecipitation of the MYC-tagged Iec1 complex, strains CH016 and CH006 were used. The complexes were captured using rabbit anti-MYC antibody coupled to agarose (Sigma) and eluted with SDS loading buffer (Bio-Rad).

***In vitro* nucleosome-remodeling assay.** Recombinant *Xenopus* histone octamers were prepared and assembled on a 12× tandem repeat of *Lytechinus variegatus* 5S rDNA as described previously (47, 79). The accessibility assay was performed as described in reference 79.

Mass spectrometry. Five microliters of eluted fractions from the FLAG-tagged Ino80 and HA-tagged Iec1 purifications, and from the corresponding mock purifications, was reduced, carbamidomethylated, and then purified using C4 ZipTips (Millipore). The purified proteins were dried by vacuum centrifugation, redissolved in 5 μl of 25 mM ammonium bicarbonate in 30% acetonitrile containing 10 ng/μl modified trypsin (Promega), and incubated overnight at 30°C. The resulting peptide mixtures were dried by vacuum centrifugation and redissolved in 5 μl of 0.1% formic acid, and 1 μl was analyzed by liquid chromatography-tandem mass spectrometry (LC-MS/MS). Bands cut from the SDS-PAGE gel were destained by washing them with 25 mM ammonium bicarbonate/50% acetonitrile (5 times) and then reduced, carbamidomethylated, and digested as described above. The tryptic peptides generated from in-solution or in-gel digestions were separated on a reversed-phase column (Vydac C_{18}; 0.05 by 50 mm; 5-μm particle size), with an acetonitrile gradient (0 to 30% over 60 min) containing 0.1% formic acid, at a flow rate of 120 nl/min. The column was coupled to a nanospray ion source (Protana Engineering) fitted to a quadrupole-time of flight (TOF) mass spectrometer (Qstar Pulsar i; Applied Biosystems/MDS Sciex). The instrument was operated in information-dependent acquisition mode, with an acquisition cycle consisting of a 0.5-s TOF scan over the *m*/*z* range of 350 to 1,500, followed by 3 2-s MS/MS scans (triggered by 2+ or 3+ ions) recorded over the *m*/*z* range of 100 to 1,700 with a 60-s dynamic exclusion of former target ions. Mass spectrometric data were searched against the eukaryote entries in Uniprot 14.2 using Mascot software (Matrix Science).

Sequence analysis. Sequence comparison was performed with BLAST and PSI-BLAST (2). The PFAM database was used for analysis of conserved domains and motifs (22).

Northern analysis. RNA was prepared with the FastRNA Pro Red Kit (MPBio) or extracted using the hot-acid–phenol method (83). Nine μg of RNA was separated on 1.2% formaldehyde agarose (FA) gels, transferred to a Hybond N+ membrane (Amersham), UV cross-linked with a Stratalinker (Stratagene), and hybridized to ^{32}P-labeled *pho4*, *pho1*, *apt1*, *cdc22*, and actin probes by the dextran sulfate method. The signal generated by the mRNA was quantified using a phosphorimager (Fuji) linked to Advanced Image Data Analysis (AIDA) software (Fujifilm) and normalized either relative to actin or relative to the ethidium bromide-stained 25S rRNA band with the AIDA software.

Quantification of mRNA levels using reverse transcription (RT) followed by quantitative real-time PCR. Hot-phenol-extracted RNA was cleaned using a Qiagen RNeasy minikit (Qiagen). To remove contaminating genomic DNA, 5 μg of isolated RNA was treated with 5 mM DTT, 2 U/μl RNasin (Promega), 1 mM $MgCl_2$, and 1 U/μg RNA DNase I (Promega). Digestion was carried out at 37°C for 30 min, and the reaction was terminated by boiling the mixture at 95°C for 5 min. One μg of DNase I-treated RNA, 100 ng random primers (Promega), and 500 μM deoxynucleotide triphosphate (dNTP) mix (Bioline) in a total volume of 20 μl were incubated at 65°C for 5 min and then cooled on ice. After a brief spin, 1× SS II buffer (Invitrogen), 10 mM DTT, and 2 U/μl RNasin (Promega) were added. The reaction mixture was incubated for 2 min at 25°C, and 200 units of SS II reverse transcriptase (Invitrogen) was added. The reaction mixture was further incubated at 25°C for 10 min and then at 42°C for 1 h. The reaction was terminated by incubation at 70°C for 15 min. The presence of specific transcripts was quantified by quantitative RT-PCR using a Bio-Rad CFX96 with SYBR green PCR Mastermix from Applied Biosystems in duplicate using the $2^{-\Delta\Delta CT}$ method (46). The primer sequences used are indicated by asterisks in Table 3.

ChIP. The chromatin immunoprecipitation (ChIP) protocol was adapted from Kurdistani et al. and Robyr and Grunstein (44, 59). At least two independent experiments were performed per strain. The cells were grown to a density of 2×10^8 cells/ml. The cells were cross-linked by adding formaldehyde to a final concentration of 1% at room temperature. The cross-linking reaction was quenched after 1 h by the addition of glycine to 0.125 M. The cells were harvested, washed in ice-cold PBS, resuspended in cell lysis buffer (0.1% SDS, 50 mM HEPES-KOH, pH 7.5, 1% Triton X, 0.1% sodium deoxycholate, 1 mM EDTA, 150 mM NaCl) with protease inhibitor cocktail (Roche), and lysed with a Fastprep machine (MPBio). The fixed chromatin was fragmented by sonication to an average size of 500 to 1,000 bp. The chromatin was immunoprecipitated with 2 μg of anti-FLAG antibody (Sigma), 5 μl anti-MYC antibody (Cell Signaling), or 5 μg of anti-histone H3 antibody (Abcam). Protein A-Sepharose beads (GE Healthcare) were washed in wash buffer (0.1% SDS, 50 mM HEPES-KOH, pH 7.5, 1% Triton X, 0.1% sodium deoxycholate, 1 mM EDTA, 500 mM NaCl). Cross-links were reversed overnight at 65°C, and protein was removed by digestion with proteinase K and phenol extraction. The purified DNA was resuspended in 40 μl Tris-EDTA, pH 8.0. The products were quantified using SYBR green I incorporation and measured using an ABI Prism 7700 Sequence Detection System (Applied Biosystems) with the primer pairs listed in Table 3. The results were corrected for background (no-antibody control) and expressed as percent chromatin immunoprecipitated from the input.

Microarray hybridization, normalization and analysis. Immunoprecipitated chromatin from two independent ChIP experiments was hybridized to GeneChip *S. pombe* Tiling 1.0FR arrays (Affymetrix). ChIP DNA was amplified to 5 μg as described previously (17, 37). Five mM dUTP was added to the second amplification (round B), and ChIP DNA was recovered with QiaQuick PCR columns. Fragmentation, labeling, and hybridization to the Affymetrix GeneChip *S. pombe* Tiling 1.0FR was performed by the Affymetrix core facility at Novum, Sweden, according to standard protocols. Duplicate raw data from Affymetrix (.CEL format) were analyzed with Tiling Analysis Software (TAS) v1.1 using quantile normalization plus scaling and run with a bandwidth of 100. The normalized data from each probe were assigned to *S. pombe* genome coordinates in TAS (*S. pombe* September 2004 genome; Sanger). The data were visualized with the Affymetrix Integrated Genome Browser. The resulting linear ratio was extracted for each probe position, defined as the center (12th) base coordinate for each 25-nucleotide probe. The 5′ and 3′ intergenic regions (IGR) were a maximum of 450 bp from the start and the stop codon, respectively, of the gene (depending on the intergenic distance between genes) and were divided into a maximum of 10 fragments of 50 bases each. Missing values were replaced by linear interpolation, using values spanning the missing data point. Values for probes of 5′ IGR positions were averaged to give one value for each promoter region. Gene ontology analysis was performed using AMIGO (http://amigo.geneontology.org/cgi-bin/amigo/go.cgi).

Western blot analysis. Proteins were separated on 4 to 12% NuPage Novex Bis-Tris gels (Invitrogen) and transferred to Hybond ECL nitrocellulose membranes (GE Healthcare). The blots were then incubated in anti-HA antibody (Roche; dilution, 1:1,000), M2 anti-FLAG antibody (dilution, 1:1,000; Sigma), or anti-MYC (dilution, 1:1,000; Cell Signaling). For the blots in Fig. 1, anti-FLAG

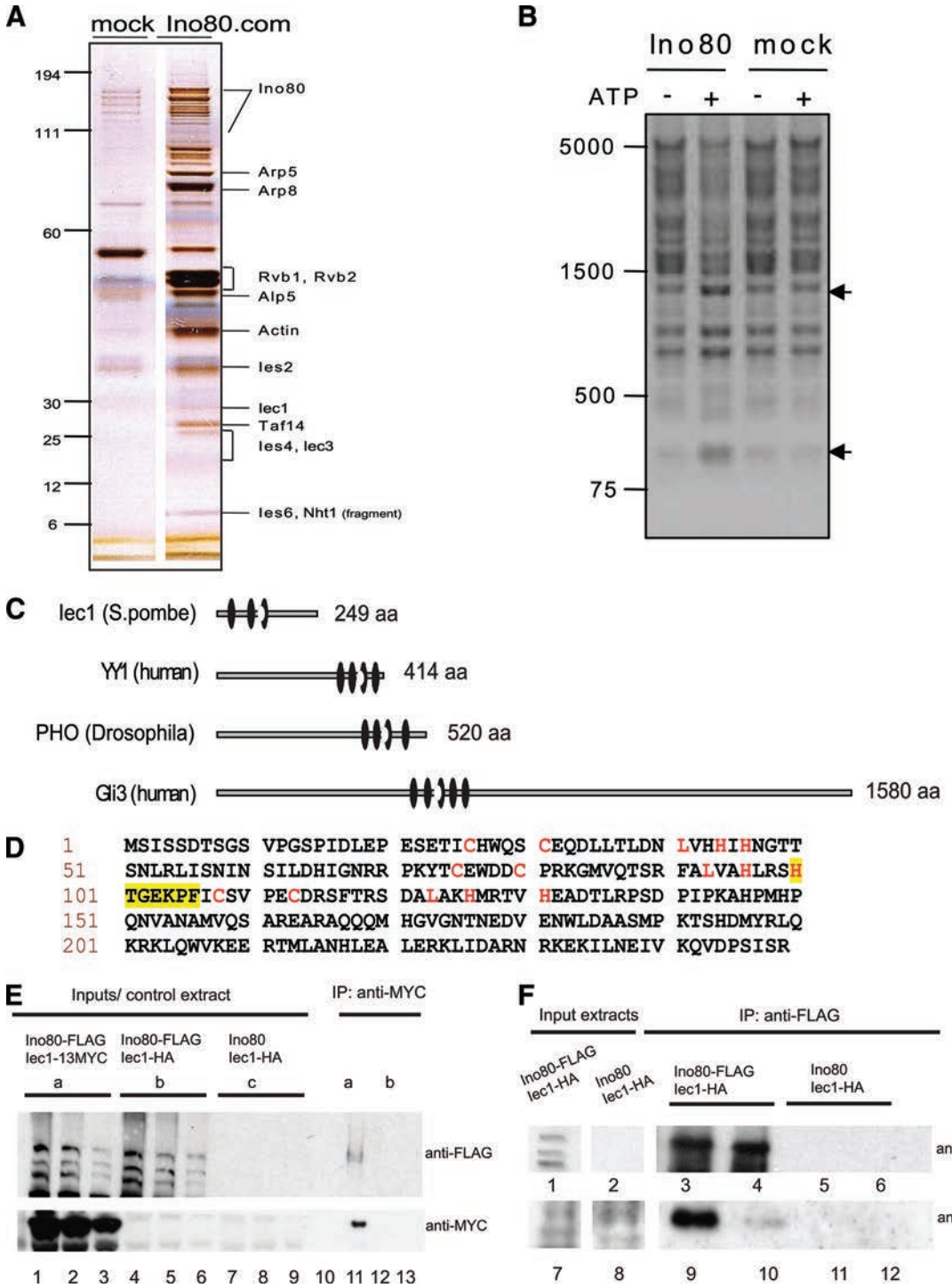

FIG. 1. Iec1 is a component of the fission yeast Ino80 complex. (A) Fractions from mock purification or Ino80 FLAG affinity purification were separated by SDS-acrylamide gel electrophoresis and stained with silver. Corresponding bands were excised and analyzed by mass spectrometry. Shown on the left are approximate protein molecular masses (kDa) and on the right the running positions of identified Ino80 complex components. (B) The fission yeast Ino80 complex remodels nucleosomes *in vitro*. Recombinant nucleosome arrays (0.5 μg) were incubated with Ino80 complex (containing ~70 fmol Arp8) or mock fractions and restriction endonuclease DraI in the presence (+) or absence (−) of ATP. The DNA was then purified, separated by agarose gel electrophoresis, and stained with ethidium bromide. Shown on the left are running positions of DNA size markers (bp); the arrows point to DNA fragments that were cleaved more readily in the presence of Ino80. (C) Schematic representations of Iec1, YY1, PHO, and GLI3. The ovals denote zinc finger domains, and the white circles are the conserved HTGEKPF motif. aa, amino acids. (D) Amino acid sequence of Iec1. Cysteines and histidines likely to be involved in forming zinc fingers are indicated in red, and the conserved HTGEKPF motif is shaded in yellow. (E) Immunoprecipitation using anti-MYC antibody from 5-ml whole-cell extracts of FLAG-tagged Ino80/MYC-tagged Iec1- (a), FLAG-tagged Ino80/HA-tagged Iec1- (b), and nontagged Ino80/HA-tagged Iec1-expressing cells (c) showed that Ino80 coimmunoprecipitated with Iec1. Lanes 1, 4, and 7 correspond to 1.5 μl crude extract; lanes 2, 5, and 8 correspond to 1 μl extract; and lanes 3, 6, and 9 correspond to

coupled to horseradish peroxidase (HRP) (Sigma) was used. The immobilized antigens were detected using enhanced chemiluminescence (ECL) techniques (Millipore).

Viability assays. Cells were grown in YES or EMM overnight at 30°C. The cells were then diluted in H_2O to a concentration of 6×10^7 cells/ml. Five 10-fold serial dilutions were prepared with H_2O, and 2 μl from each dilution was spotted onto agar plates. Photographs were taken 3 to 5 days after spotting.

Plasmid loss assay. A control strain with empty vector (CH008) and an *ino80* null strain complemented with a plasmid driving expression of Ino80 in *trans* (SA003) were inoculated in 100 ml nonselective rich medium (YES) and grown overnight. One ml of this culture was used to inoculate a fresh 100-ml culture, and the process was repeated two more times. Approximately 1,000 cells were plated onto nonselective (NS) rich medium and selective medium (minus Leu) and incubated at 30°C.

Microscopy. Cells were grown in EMM or low-phosphate or low-adenine EMM for 4 days. The cells were DAPI (4′,6′-diamidino-2-phenylindole) stained and imaged using an Olympus BX40 microscope. Two hundred cells each of the wild-type (WT), Δ*iec1*, and Δ*iec1* plus pIec1 strains grown in either EMM, low-phosphate EMM (EMM/low P_i), or EMM/low adenine were scored as either ascus or vegetative, and the percentage of asci was calculated.

Nucleotide pool measurements. Nucleotide pools were measured in freshly grown cells using an enzymatic method derived from reference 66 and modified as described in reference 48.

Yeast cells were harvested in mid-log phase, with about 10^8 cells used for each extraction. Duplicate extractions were done for each experiment, and the data shown are based on three different experiments. The cells were centrifuged, and the pellet was resuspended in 3 ml of ice-cold 60% aqueous methanol. Each suspension was held at −20°C for 1 h, followed by centrifugation. The supernatants were removed, and each pellet was washed with 1 ml 60% methanol. The washes were added to the original supernatants, and then each solution was held in a boiling water bath for 3 min. This was followed by centrifugation for 15 min at 17,000 × *g*. Each supernatant was transferred to a fresh tube and taken to dryness under vacuum. Each residue was dissolved in water and stored at −20°C for later analysis. Reaction mixtures (50 μl) contained 100 mM HEPES buffer, pH 7.5, 10 mM $MgCl_2$, 0.1 unit of *Escherichia coli* DNA polymerase I Klenow fragment (United States Biochemical), 0.25 μM oligonucleotide template, and 0.67 μM [^{3}H]dATP (30 Ci/mmol; 1.0 μCi per assay; Amersham Biosciences) or [^{3}H]dTTP (PerkinElmer Life Sciences). Incubation was carried out for 60 min at 37°C. Deoxyribonucleotide pools were expressed as mole amount per mg yeast protein.

Microarray data accession number. Tiling data are available on MIAMexpress (http://www.ebi.ac.uk/microarray/) under accession number E-MEXP-2284.

RESULTS

The fission yeast Ino80 complex is highly conserved. We identified the fission yeast ORF SPAC29B12.01 as the Ino80 homologue by sequence homology analysis. The endogenous Ino80p was FLAG tagged, and the associated complex was affinity purified. Mass spectrometric analysis revealed highly conserved core complex a similar to the budding yeast and mammalian Ino80 complexes (Fig. 1A and Table 4). Ino80 copurifies with seven proteins that have homologues in both budding yeast and humans (36, 42, 43, 50, 65): SPAC664.02 (homologue of budding yeast ARP8), SPBC365.10 (ARP5), SPAPB8E5.09 (RVB1), SPBC83.08 (RVB2), Alp5 (ARP4), SPAC222.04 (IES6), and SPAC6B12.05 (IES2).

In addition to this "core complex," fission yeast Ino80, like its budding yeast counterpart but unlike the human Ino80 complex, contains (i) an HMG box-like protein (SPAC10F6.08) with similarities to the NHP10 protein of budding yeast, which has been found to be involved in DNA damage repair (52); (ii) the TATA binding protein-associated factor Taf14/Tfg3; and (iii) actin (36, 65). We also identified several uncharacterized proteins that are unique to the fission yeast Ino80 complex: SPCC1259.04, SPCC16C4.20, SPAC23G3.04, and SPAC144.02 (Table 4). A comparative proteomic analysis of yeast chromatin modification and remodeling complexes identified most fission yeast Ino80 complex subunits presented here without further functional analysis (67). However, there are also notable differences between our study and that of Shevchenko et al. We assigned Taf14/Tfg3 and the gene product of SPCC16C4.20 as potential Ino80 subunits. Taf14/Tfg3 (the gene product of SPAC22H12.02) was clearly identified in our Ino80-FLAG pulldown (Fig. 1A) and is the predicted orthologue of *S. cerevisiae* TAF14. This protein is also called SWP29, TAF30, TFG3, and ANC1 and is a subunit of the S. *cerevisiae* Ino80 complex subunit (63). It has also been shown to be a subunit of the general transcription factors TFIIF and TFIID and the SWI/SNF complex (11, 30, 31, 40). Unlike Shevchenko et al., we did not identify Iec5p and Pht1p (the fission yeast orthologue of histone variant H2AZ). These differences may be related to the distinct purification protocols (affinity purification using the FLAG tag versus TAP) and growth conditions of the two studies.

We tested whether the purified Ino80 complex exhibits ATP-dependent nucleosome-remodeling activity *in vitro*. Nucleosomal arrays were assembled with recombinant purified histones. In the presence of the purified Ino80 complex and ATP, there was increased cleavage of the chromatin by the restriction enzyme DraI compared to controls, indicating that Ino80 remodels nucleosomes to render chromatin more accessible (Fig. 1B).

The novel zinc finger protein Iec1 is associated with the fission yeast Ino80 complex. The fission yeast Ino80 complex contains a novel zinc finger protein, Iec1, encoded by the previously uncharacterized open reading frame SPAC144.02 (Fig. 1A and Table 4) (67). Sequence homology analysis indicated that this 249-amino-acid protein contains two C_2H_2-type zinc finger motifs and a possible zinc finger at its N terminus (Fig. 1C and D) (22). Our analysis revealed no apparent *S. cerevisiae* orthologue for the protein, but similarity to the zinc finger motifs of the GLI-Krüppel family of transcription factors was found (Fig. 1C). The *Drosophila* PcG PHO and its mammalian orthologue YY1 have been found associated with Ino80 (10, 41, 82). These proteins belong to the GLI-Krüppel family and show similarity to SPAC144.02 at the level of their C_2H_2 zinc finger motifs (Fig. 1C). Furthermore, a

0.5 μl extract. Lane 11 corresponds to 13% of the immunoprecipitation eluate from the extract of FLAG-tagged Ino80/MYC-tagged Iec1-expressing cells, lane 13 shows the corresponding control eluate from the extract of HA-tagged Ino80/MYC-tagged Iec1-expressing cells, and lanes 10 and 12 are blank. The immunocomplexes were subjected to immunoblot analysis with the indicated antibodies. The Western blot also shows that Ino80-FLAG was specifically detected, because there was no band when Ino80 was not FLAG tagged (lanes 7 to 9). (F) Immunoblot analysis of an anti-FLAG antibody immunoprecipitation experiment from whole-cell extracts of HA-Iec1/FLAG-Ino80-expressing cells. The control immunoprecipitation was done with extracts from cells expressing HA-Iec1 and nontagged Ino80. Lanes 1, 2, 7, and 8 show the inputs (1-μl extracts; 0.0002% of the total input); lanes 3 and 4 show the anti-FLAG blots from 0.2 and 0.1 μl of immunoprecipitates from HA-Iec1/FLAG-Ino80-containing extracts (total eluate, 200 μl); and lanes 5 and 6 show the corresponding controls. Lanes 9 and 10 show the anti-HA blots from 3 and 1 μl of immunoprecipitates from HA-Iec1/FLAG-Ino80-containing extracts, and lanes 11 and 12 show the corresponding controls.

TABLE 3. Quantitative-PCR primer pairs

Locus	Sequence	
	Sense primer	Antisense primer
pho1	5′-CGTTCATGCCTACATCTTAATACAGG-3′	5′-ACTACCGCGTAGCGATGAGAA-3′
	5′-TTGGAACGGCAATGTGCTAGT-3′	5′-GCAGAGTGCGAACATGAGACC-3′
	5′-TTAAGGTAGCGTTCAATGTTCTTGC-3′	5′-ATTCAGCGAACTGAGCGTTG-3′
	5′-GACATGGTTCTCGTAATCCTACCG-3′[a]	5′-CAATAGGAACTGATCCATTAAGCAAT-3′[a]
	5′-CAACTTGGACTCCTGTTATTGAAGC-3′	5′-AGAGCTCATGGTAACGCTCGTAA-3′
	5′-TTACGAGCGTTACCATGAGCTC-3′	5′-GAATCTACAACGCGCTGCTG-3′
	5′-TCAGAGAATGCTACTGCTGGATC-3′	5′-TTCTCCAAGCTTCGAGAGCA-3′
	5′-CCTGCTCTCGAAGCTTGGAG-3′	5′-CGTCGTTGGTAAGATTATAGTTGGAA-3′
	5′-TCCAACTATAATCTTACCAACGACGA-3′	5′-CTTACAGAATTCGCTATAGTCTTGAA-3′
	5′-GAGGTGCCTATGCTAATAGCCTTG-3′	5′-CAACAGGAATAATATTGGCATCATG-3′
	5′-CTTCCTACCAAGTCCACTCTCACTC-3′	5′-GCGGACATAGTACTTAGAATCTTCAC-3′
	5′-GCCATCTTGTTAACGAGGAGGT-3′	5′-AGGCGTACAACTCACACATACCA-3′
	5′-ATGGTATGTGTGAGTTGTACGCCTA-3′	5′-AGCAGCCACAGCACTAGCATT-3′
	5′-AACCTATACGTGCACAACGTTGT-3′	5′-GGTATCGCGTAATTAGTCATCTCTTC-3′
pho4	5′-AGATAGCAGACTAATACTCTTCAATGCC-3′	5′-TTGTACGAGCTGCTACATAATATTGC-3′
	5′-TCCAATGTAGTCGTGCCGAA-3′	5′-AAGCGCAAGAAGCAGCAGAT-3′
	5′-AAGTTCGTTGATTGAATAGACTACCG-3′	5′-TGTATGAATCAACCAACGACCAG-3′
	5′-CATCCATCGTTCATGCTGGTA-3′	5′-CATGATATACACTAATCGTTCCAAGATG-3′
	5′-AGGACCATCTTGGAACGATTAGTG-3′	5′-GATCCATGACGCTGAAGCAA-3′
	5′-AATGCCGACCAGTTGTCCAG-3′	5′-GAGCAGCAGTATTGATATCGTAGACATC-3′
	5′-GATGTCTACGATATCAATACTGCTGCTC-3′	5′-CGGAAGAACGATGAAGTTGGTT-3′
	5′-AGCCTATCGCCAATCGCTTA-3′	5′-TCGCTGTTATCTCTGAGAGCGA-3′
	5′-GTGTGAATAATGCTTCCGATCGT-3′	5′-AAGAGCAGCCTCGACTGGAAT-3′
	5′-CCATTAGAGGTAGAATTAACACGAACC-3′	5′-TTACTGATTGCGGTTATGGTCCT-3′
	5′-TTGTGTCGTTCGTGTGTGTGGTAA-3′	5′-TCTCAAGATATAACGCGTACATTAACG-3′
	5′-AACCAGCTATCCGGAATTACCA-3′	5′-ACACATGCGGTAATCAGATGAGTT-3′
apt1	5′-GAACGGAGAGAAGGAGCGAT-3′	5′-AATCTTACGCCTCTACATTACTCGTT-3′
	5′-TAATGATGAACAACGGATATGACTGAA-3′	5′-AACTGTCAGCCACAACTCCATGT-3′
	5′-TTCGCTGCATAGACGGTAACG-3′	5′-AGGTAATTGATTCTATCGTCGGACA-3′
	5′-GAGGTTGGATAGGAACGGTGA-3′	5′-TTAAGCAATTGCAAGGCGTAA-3′
	5′-TTGGTCGTCGTAAGCTACAATAAGG-3′	5′-CCACCAGTAGCAAGAATGTCGTC-3′
	5′-GTTGACGACATTCTTGCTACTGGT-3′	5′-GGAAGAGATGTCCAACTAATTCACC-3′
	5′-CGTAAGCGTCTTATGGCTCCTACT-3′	5′-ATTCACTACCATCAGGTGCTTCATC-3′
	5′-ATATGACCGCAAGTCTATACACATGC-3′	5′-TCGTACTTCCAAGGAACTCCAGTT-3′
	5′-CATCCGTGATGAGAATTAACAATCC-3′	5′-GCTCCACTTGGCAACTGCTC-3′
	5′-GGGAATCTTGTTTGAAGATATAATGCC[a]	5′-CCAACAATCACATCAATGTTATTGA-3′[a]
aah1	5′-AGATTCACCAGACATGATTACTGAGTG-3′	5′-TTCATCACGACATGGCCAAT-3′
	5′-GAAGTTGTCAAGAGTGTTGCTGCT-3′	5′-ATCGCTCCATCCGTTACACC-3′
	5′-AATGCGAGCATCATGTGCAT-3′	5′-CGCAGCATCATCACTAGGAAGA-3′
	5′-TGCTGTGTCTGTGTTGATTGAGG-3′	5′-TGAACTCCTTGTGAATGAGCGAT-3′
	5′-TCTGCGTCACTTGCCTTCTG-3′	5′-CCTGCAACAATTCCATTCTCAA-3′
	5′-GCAGGTGAAGAAGGTGATCCA-3′	5′-TCTGCAACTCGCTTCATTAACTCT-3′
	5′-GAGTTAATGAAGCGAGTTGCAGAAG-3′	5′-GGCAATAGAATTGACACAACGAAGT-3′
	5′-GGCGGTTACACCTTGGAGAA-3′	5′-GCCGTTGATAGCAGCATTAGC-3′
	5′-AATGAGCAGGCCATGTTAACATC-3′	5′-CCTGAAGACCTAGCCAGCCAT-3′
ade1	5′-TTGTGCTCGCATCTGGAATG-3′	5′-GTAATGTACAATATCGCTGCATCGTT-3′
	5′-CGGTCGTGAACATACCATCG-3′	5′-AGATTCCGCTCCATTGCTTG-3′
cdc22	5′-GTTCAATCTCATAGAGCAGGTTGGTAG-3′	5′-TACGCGTCTCAATTGCAACG-3′
control	5′-CCTTCCGTCCTCTATGCCATC-3′	5′-TCAATAATCATCTTACAAGACCGGAA-3′
actin	5′-CCCCAAATCCAACCGTGAGA-3′[a]	5′-GGCATACAAAGACAAAACAGCTTG-3′[a]
iec1	5′-TGCTCAGTGCCAGAGTGTGATAG-3′[a]	5′-GGTCCGAAGGCCGTAGTGTA-3′[a]

[a] Used for RNA quantification.

short stretch of 7 amino acids, HTGEKP(F), a motif present in all YY1 proteins across species and GLI-Krüppel family members, was found in SPAC144.02 (Fig. 1D) (in GLI3, we found HTGE KPH).

The presence of Iec1 in the Ino80 complex was confirmed by coimmunoprecipitation experiments with whole-cell extracts from endogenously MYC-tagged or HA-tagged Iec1- and FLAG-tagged Ino80-expressing strains, followed by Western

TABLE 4. Comparison of *S. pombe*, *S. cerevisiae* and human Ino80 complexes

S. pombe	*S. cerevisiae*[a]	Human[b]	Description
Ino80 (SPAC29B12.01)[e]	**INO80**	**hIno80**	**SNF-like helicase**
Arp8 (SPAC664.02)	ARP8	Arp8	Actin-related protein
Arp5 (SPBC365.10)	ARP5	Arp5	Actin-related protein
Alp5	ARP4	BAF53a/Arp4	Actin-related protein
Rvb1 (SPAPB8E5.09)	RVB1	TIP49a	AAA^+ ATPase
Rvb2 (SPBC83.08)	**RVB2**	**TIP49b**	**AAA^+ ATPase**
Ies6 (SPAC222.04)	IES6	C18orf37	Related to YL-1 family
Ies2 (SPAC6B12.05)	IES2	PAPA-1	PAPA_1 domain
Iec1		**YY1**	**Zinc finger transcription factor**
HMG-box like protein (*nht1*)	NHP10		HMG-type domain; binds DNA
Taf14/tfg3	TAF14		Transcription factor
Act1	**ACT1**		**Actin**
SPAC23G3.04 (*ies4*)[c]	IES4		Ino80 complex subunit
SPCC1259.04 (*iec3*)[c]			Sequence orphan
SPCC16C4.20[c,d]			Sequence orphan
	IES1		Ino80 complex subunit
	IES3		Ino80 complex subunit
	IES5		Ino80 complex subunit
		Amida/TCF3	b-ZIP-type protein; DNA binding
		NFRKB	Metazoan specific; nuclear factor
		MCRS1	Forkhead-associated domain protein
		FLJ90652	Conserved in metazoa
		FLJ20309	Conserved in metazoa
		UCH37	Ubiquitin C-terminal hydrolase

[a] From reference 65.
[b] From reference 36.
[c] Requires further validation.
[d] Unique to this study.
[e] Boldface entries are found also in the Iec1-HA pulldown (and corresponding homologues in other Ino80 complexes).

blot analysis (Fig. 1E and F). HA-tagged Iec1 was used to coimmunoprecipitate associated proteins from whole-cell extracts, followed by mass spectrometric analysis. Iec1 copurified with Ino80, the AAA^+ ATPase Rvb2, and actin in what appeared to be an Iec1-Ino80 core complex (Table 4). This complex appears similar to the YY1/PHO-Ino80 complexes in mammalian cells and *Drosophila*, which contain YY1/PHO, Ino80, Rvb1/2, actin (only in *Drosophila*), and Arp5/Arp8 (Table 4) (10, 41, 82). We concluded that the fission yeast Ino80 interacts with Iec1, a novel C_2H_2 zinc finger protein related to GLI-Krüppel family members, such as YY1, and that the protein forms a core complex with Ino80 resembling the YY1-Ino80 core complexes of higher eukaryotes.

Iec1 and subunits of the Ino80 complex are involved in replication and the DNA damage response. The disruption of the budding yeast Ino80 complex impairs DNA repair, replication, and transcription (reviewed in references 4 and 77). We wanted to establish if the fission yeast complex also plays a role in these processes. In a plasmid loss assay, a strain with the endogenous *ino80* deleted and with a plasmid expressing Ino80 in *trans* retained the plasmid for survival. This indicates that Ino80 is essential for cell viability (Fig. 2A). A spore viability assay supported this finding, because *ino80* mutant spores did not germinate after ascus dissection of $ino80^{-/+}$ diploid cells (data not shown). The *arp8*, *nhp10*, *ies2*, and *ies6* subunits of the Ino80 complex were deleted without loss of viability. The responses of Δ*arp8*, Δ*ies2*, Δ*ies6*, and Δ*nhp10* mutant cells to DNA replication stress and DNA damage were tested by plating serial dilutions of each strain onto plates containing the drug HU or bleocin or exposing the plates to UV irradiation and assaying viability and growth. HU sensitivity indicates an impaired response to replication stress, as the drug depletes deoxyribonucleotide pools, resulting in stalled replication forks (8, 57). Bleocin causes single- and double-strand DNA breaks (53, 65). UV irradiation leads to the formation of pyrimidine dimers and other DNA damage (70). Δ*arp8* and Δ*ies2* cells, but not Δ*nhp10* cells, were sensitive to HU, bleocin, and UV irradiation compared to wild-type cells (Fig. 2B). As the Δ*ies6* mutant could not grow on minimal medium, it was plated on rich medium (YES), where it was also sensitive to HU, bleocin, and UV irradiation (Fig. 2C). Thus, the fission yeast Ino80 complex is required for the DNA damage and DNA replication stress responses. We then tested whether Δ*iec1* shows similar phenotypes in the presence of HU and bleocin or after UV irradiation. Under all conditions, the deletion of *iec1* severely decreased cell viability (Fig. 2D). Expression of Iec1 in *trans* in the Δ*iec1* background improved survival (Fig. 2D). Therefore, there is a functional interaction between Iec1 and the Ino80 complex, as Iec1 and the subunits Arp8, Ies2, and Ies6 of the Ino80 complex are required for the physiological response to DNA damage and replication stress.

Iec1 and the Ino80 complex are involved in nucleotide metabolism. To explore the functions of Iec1 in addition to its role in DNA repair/replication stress, we tested the viability of wild-type and Δ*iec1* strains under various conditions. We found that Δ*iec1* strains do not grow well at high temperature (37°C); in 1% formamide; in 0.5 mM $CdSO_4$, a heavy metal; in 10 μg/ml benomyl, a microtubule inhibitor; and in 0.004% methyl methanesulfonate (MMS), a DNA-alkylating agent (Fig. 3A).

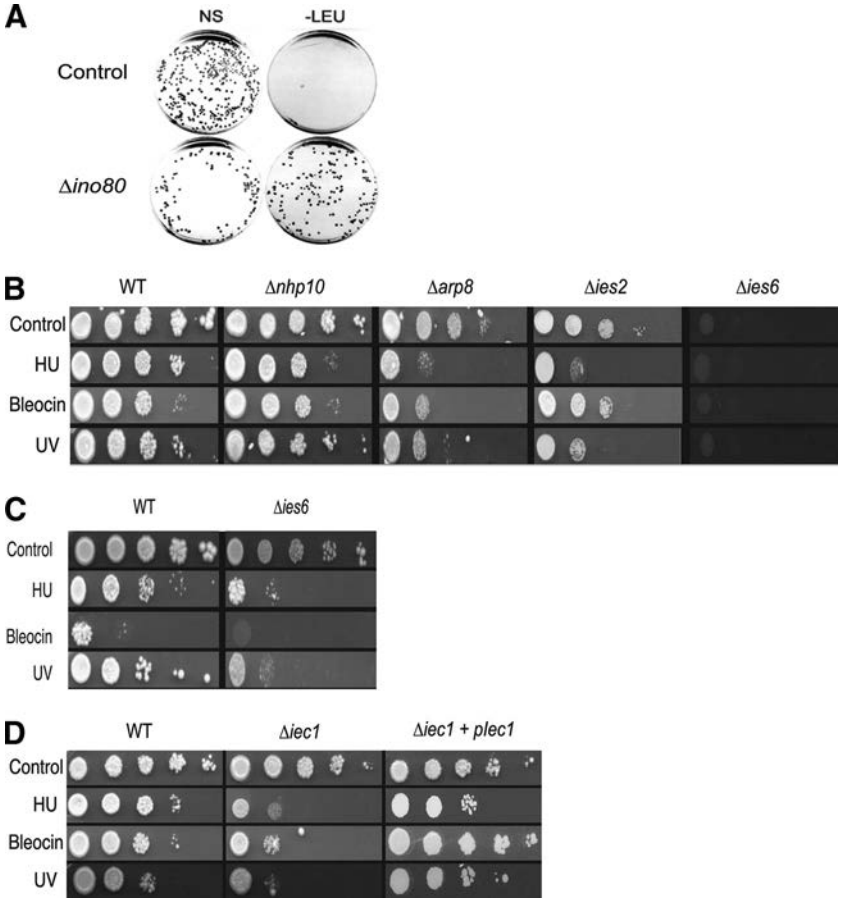

FIG. 2. Ino80 complex subunits are required for viability and the response to DNA damage and replication stress. (A) Plasmid loss assay demonstrating the essential role of *ino80* in fission yeast. *ino80* null cells complemented with a plasmid expressing Ino80 in *trans* (SA003) retained the plasmid for survival, whereas the control cells with empty vector (SA002) lost the plasmid and became auxotrophic for leucine. NS, nonselective medium containing leucine. (B) Tenfold serial dilutions of a control strain (WT; FY367), *nhp10* null mutants (Δ*nhp10*; CH010), *arp8* null mutants (Δ*arp8*; CH011), *ies2* null mutants (Δ*ies2*; CH012), and *ies6* null mutants (Δ*ies6*; CH013) were plated on minimal medium (EMM) containing 7.5 mM HU or 3 μg/ml bleocin or were exposed to 100 J/m^2 UV light (UV), incubated at 30°C, and visualized after 5 days. (C) Δ*ies6* cells were plated on rich medium (YES) and exposed to the same conditions as in panel B. (D) Tenfold serial dilutions of a control strain with empty vector (WT; CH008), an *iec1* null mutant with empty vector (Δ*iec1*; CH009), and an *iec1* null mutant with vector containing full-length Iec1 (Δ*Iec1*+pIec1; CH007) were plated as in panel B.

Δ*iec1* cells showed altered phenotypes when grown under low-phosphate or low-adenine conditions (Fig. 3B). When intracellular adenine levels are low, the de novo adenine synthesis pathway is activated. Due to a mutation in *ade6* in the experimental strain, the pink pigment 5′-phosphoribosyl-5-aminoimidazole (AIR), a purine precursor, accumulated (Fig. 3C). Unlike wild-type cells, Δ*iec1* cells grown in low-phosphate rich medium (YES) accumulated this pink pigment (Fig. 3B). This indicates a switch from salvage to de novo AMP biosynthesis (58). Since the pink pigment is seen upon phosphate starvation when the adenine supply is not limited, this suggests that the *de novo* biosynthesis pathway is being erroneously activated in Δ*iec1* cells. It also indicates cross talk between phosphate and purine metabolic pathways in the cell. In line with this, Δ*iec1* cells grow well in low-adenine rich medium (YES), but unlike wild-type cells, they do not turn pink (Fig. 3B). Therefore, the switch from adenine salvage to the de novo pathway is not correctly regulated in Δ*iec1* cells.

Having established that deletion of *iec1* affects phosphate and adenine metabolism, we investigated whether other components of the Ino80 complex were also involved in these pathways. We found that Δ*arp8*, Δ*ies6*, and Δ*ies2* cells cannot grow on phosphate-depleted medium, whereas Δ*nhp10* cells remain viable (Fig. 3B). Δ*arp8*, Δ*ies6*, and Δ*ies2* cells also failed to turn pink in low-adenine medium (Fig. 3B). As the deletion of *iec1*, *arp8*, *ies2*, or *ies6* produced the same phenotype, this suggests that these proteins act together in a common pathway. The mutant with a double deletion of *iec1* and *ies2* (Δ*iec1* Δ*ies2*) retained the ability to turn pink under low-adenine conditions and was viable in low phosphate, whereas the single- deletion mutants were not (Fig. 3B). This finding confirmed that Iec1 functions with the Ino80 complex and may suggest that Iec1 and Ies2 control one another (see Discussion).

Meiosis and subsequent sporulation are normal responses of fission yeast upon nutrient deprivation. To determine if this pathway was affected, cells were grown on minimal medium (EMM), EMM/low P_i, or low-adenine EMM and

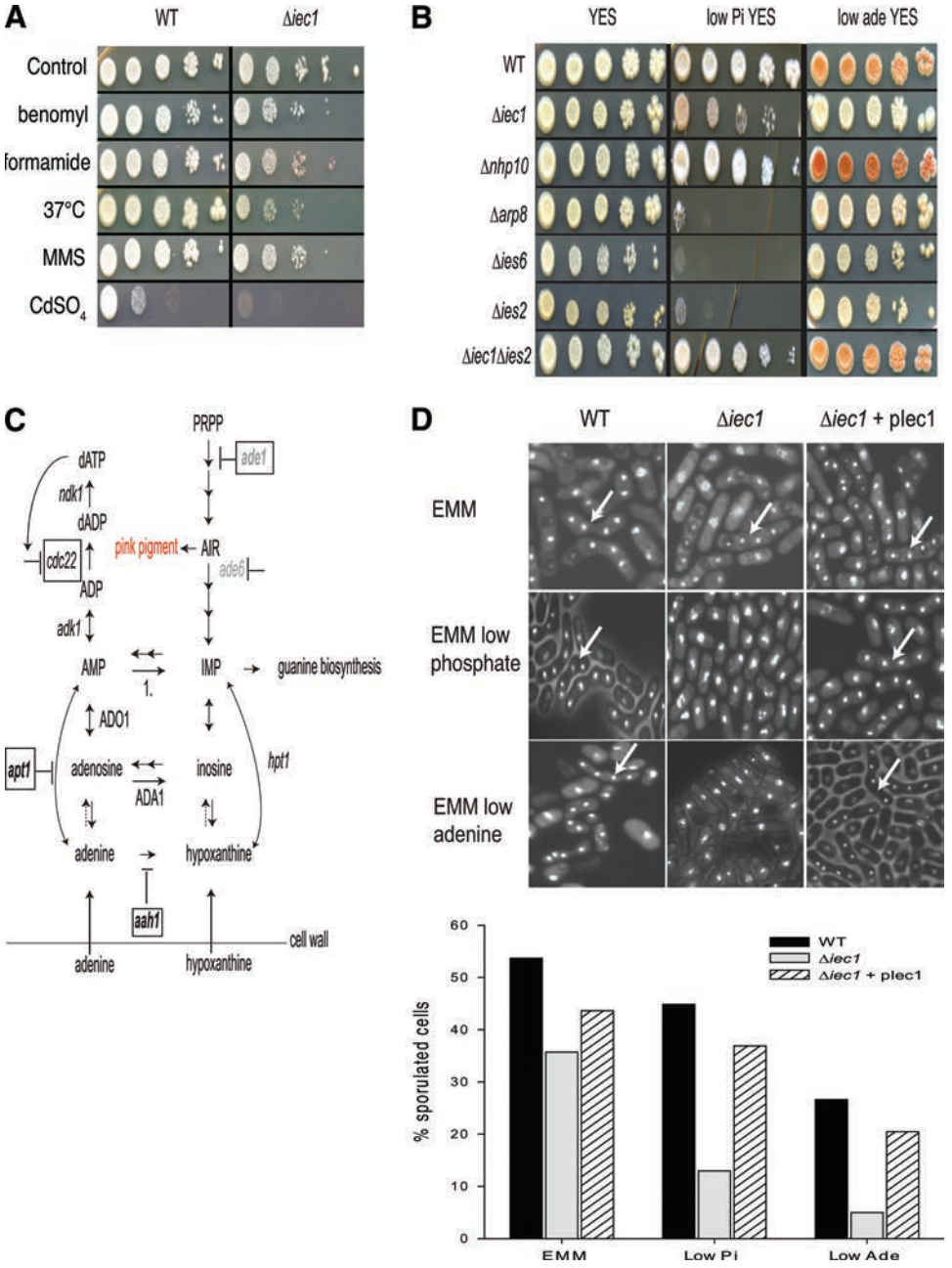

FIG. 3. Fission yeast strains lacking *iec1* and Ino80 complex subunits are sensitive to various stress conditions, including phosphate and adenine limitation. (A) Tenfold serial dilutions of control (WT; FY367) and Δ*iec1* (CH015) were plated on rich medium (YES) and incubated at 37°C or supplemented with 10 μg/ml benomyl, 1% formamide, 0.004% MMS, or 0.5 mM $CdSO_4$; incubated at 30°C; and visualized after 3 to 4 days. (B) Dilutions of control (WT; SA001), Δ*iec1* (CH003), Δ*nhp10* (CH010), Δ*arp8* (CH011), Δ*ies6* (CH013), and Δ*ies2* (CH012) cells and *iec1 ies2* double-deleted (Δ*iec1*Δ*ies2*; CH014) cells were plated onto YES, phosphate-depleted YES, and low-adenine YES; incubated at 30°C; and visualized after 3 to 4 days. (C) Schematic of the de novo and salvage pathways of adenine biosynthesis (72). The fission yeast enzymes are in lowercase italics, and the human and budding yeast genes are in uppercase. *ade1*, adenylate deaminase; gray, de novo synthesis pathway; boxed, enzymes in the pathway found to be affected by the deletion of *iec1* in this study. (D) (Top) Control cells with empty vector (WT; CH008), Δ*iec1* cells with empty vector (CH009), and Δ*iec1* plus pIec1 cells (CH007, expressing full-length Iec1 in *trans*) were grown in EMM, low-phosphate EMM, and low-adenine EMM; stained with DAPI; and visualized by light microscopy. Asci containing 4 spores can be seen in EMM, but not low-phosphate EMM or low-adenine EMM, in the Δ*iec1* cells (arrows). (Bottom) Diagram showing the percentages of asci within the cell populations depicted in the images above.

then stained with DAPI and visualized using fluorescence microscopy to detect asci (Fig. 3D). In wild-type cells, asci were detected under all conditions. However, upon *iec1* deletion, the sporulation frequency dropped severely in low-phosphate or low-adenine EMM. This could be rescued by expressing Iec1 in *trans*, indicating that the presence of Iec1 is required for efficient sporulation when cells are deprived of either phosphate or adenine.

Iec1 is required for the expression of genes involved in adenine and phosphate metabolism. We wanted to establish if the sensitivity to low levels of phosphate and adenine seen in the *iec1* mutants was due to a direct effect on phosphate-responsive genes and those involved in adenine metabolism. Deletion of Ino80 in budding yeast causes repression of phosphate-responsive genes, such as the PHO5, PHO12, and PHO89 genes, as well as the adenine metabolism genes AAH1 and ADK1 (64, 71, 76). We tested the effect of Iec1 deletion upon the expression of *pho1* and *pho4*, the only two acid phosphatase genes in fission yeast. These genes correspond to the budding yeast PHO5 and PHO3 genes, respectively (49, 60). Pho4 is a constitutive acid phosphatase repressed specifically by thiamine (49, 60). Pho1 is weakly repressed by phosphate, adenine, and thiamine (49, 60, 61). We also tested the expression of *apt1*, encoding adenine phosphoribosyltransferase 1, an enzyme in the salvage pathway that catalyzes the conversion of adenine to AMP (Fig. 3C). Northern blot analysis showed that the mRNA levels of all three genes were not affected in Δ*iec1* cells when the cells were grown at normal phosphate levels (Fig. 4A and data not shown) but were significantly downregulated in low phosphate in Δ*iec1* cells compared to control cells (Fig. 4A and B). This indicates that, upon phosphate starvation, Iec1 is necessary for the correct expression of genes involved in phosphate response and adenine metabolism. We tested the expression of Iec1 and found that is was markedly upregulated upon phosphate starvation, consistent with a role in regulating the response to this nutritional stress (Fig. 4C).

Ribonucleotide reductase (RNR) is a key enzyme in deoxyribonucleotide metabolism that converts ribonucleotides into deoxyribonucleotides (55). Transcriptional upregulation of the RNR genes is known to occur upon DNA damage (12, 20). In fission yeast, active RNR is a heterotetramer of two large (Cdc22) and two small (Suc22) subunits (21). *cdc22* mRNA levels decreased in the *iec1* mutant in EMM and, to a lesser degree, in EMM/low P_i (Fig. 4D). We tested *cdc22* expression in cells treated with HU, a condition that in budding yeast leads to upregulation of RNR expression, which is not affected by deletion of *INO80* (52, 84). Deletion of *iec1* did not affect the upregulation of *cdc22* in cells treated with HU (data not shown). We measured deoxyribonucleoside triphosphate pools in wild-type and *iec1* mutant cells in EMM and EMM/low P_i and found that, while dCTP and dGTP levels did not change markedly, the dTTP pool increased at the expense of the dATP pool in *iec1* mutant cells compared to wild-type cells (Fig. 4E). These results are consistent with partial inhibition of RNR, as this decrease in dATP and increase in dTTP has been reported in mouse 3T6 cells treated with the ribonucleotide reductase inhibitor HU (8). These observations suggest that the Iec1-Ino80 complex is required for optimal expression of *cdc22* under normal and phosphate-depleted growth conditions but that in the presence of HU other activities may override the requirement for Iec1-Ino80.

Ino80 is targeted to promoters of phosphate-responsive genes upon phosphate starvation. To test the direct involvement of Ino80 in the regulation of the phosphate-responsive and nucleotide metabolism genes, we performed chromatin immunoprecipitation, followed by hybridization analysis to high-density tiling arrays with 20-bp resolution. Immunoprecipitated Ino80-bound chromatin fragments were isolated from cells grown in EMM or EMM/low P_i. The genome-wide analysis revealed significant differences in Ino80 binding between low and normal phosphate levels. There was a substantial increase in the number of promoter regions (5′ intergenic regions) that showed Ino80 enrichment during phosphate starvation (Fig. 5A), suggesting a role for Ino80 in low-phosphate stress response. Gene ontology analysis of Ino80 promoter targets revealed that a significant number of the genes targeted in low phosphate are involved in the stress response (Fig. 5B). The ChIP-on-chip analysis showed that there was an accumulation of Ino80 at the promoters of *apt1*, *ade1*, *aah1*, *pho1*, and *pho4* upon phosphate starvation (Fig. 5C). *aah1* encodes adenine deaminase, which deaminates adenine to hypoxanthine, and *ade1* is a gene involved in the de novo synthesis pathway (Fig. 3C). The increase of Ino80 accumulation at the *cdc22* promoter was less pronounced, consistent with our finding that Iec1 regulates *cdc22* in phosphate-containing and phosphate-depleted media (Fig. 5C). However, there was a notable increase in Ino80 binding to the *suc22* promoter upon phosphate starvation (data not shown). Other genes involved in adenine metabolism exhibiting a substantial increase of Ino80 binding during phosphate starvation were *ade3*, *ade4*, and *prs1* (ribose-phosphate pyrophosphokinase) (data not shown). In conclusion, phosphate starvation invokes a stress response upon which Ino80 binds to a large number of promoters, including those of genes that we have shown to be downregulated when *iec1* is deleted.

Iec1 is required for the binding of the Ino80 complex to target genes. We examined whether deletion of *iec1* causes a decrease in the occupancy of the Ino80 complex at the *pho1* gene. We addressed this by chromatin immunoprecipitation of FLAG-tagged Ino80 protein in wild-type and Δ*iec1* cells grown in normal and low-phosphate EMM, followed by quantitative PCR. In cells grown in minimal medium with normal phosphate levels, *iec1* deletion did not significantly affect Ino80 occupancy at *pho1*; if anything, it led to some increased occupancy (Fig. 6A, left). However, in low phosphate, Ino80 occupancy at *pho1* was dependent on Iec1 (Fig. 6A, right). We also examined the role of Iec1 for binding of Ino80 to the *pho4*, *apt1*, *aah1*, and *ade1* promoters. In line with the notion that Iec1 is important for binding of Ino80 to these genes in low phosphate, we found that the occupancy of Ino80 decreased at these loci upon the deletion of *iec1* but not at the promoter of the control *ade10* gene upon phosphate starvation (Fig. 6B).

The presence of Ino80 at the *cdc22* promoter decreased in *iec1* mutant cells grown in normal and low phosphate, suggesting that the Iec1-Ino80 complex is required for correct *cdc22* regulation. This is in line with our observation that Iec1 is important for *cdc22* mRNA expression irrespective of phosphate levels in the medium (Fig. 6C). These results are different from the results in budding yeast, where Ino80 does not appear to regulate RNR gene transcription (52).

Next, we asked if Iec1 is targeted to the phosphate and nucleotide metabolism genes and if it binds to specific sequence elements, e.g., over the promoters, by performing chromatin immunoprecipitation experiments for Iec1 at the *pho1*, *pho4*, *apt1*, and *aah1* loci with cells grown in low-phosphate media. We found Iec1 broadly distributed over the bodies of the genes with no indication that it binds specific sequence elements (Fig. 7A to D).

We concluded that the Ino80 complex is recruited to genes

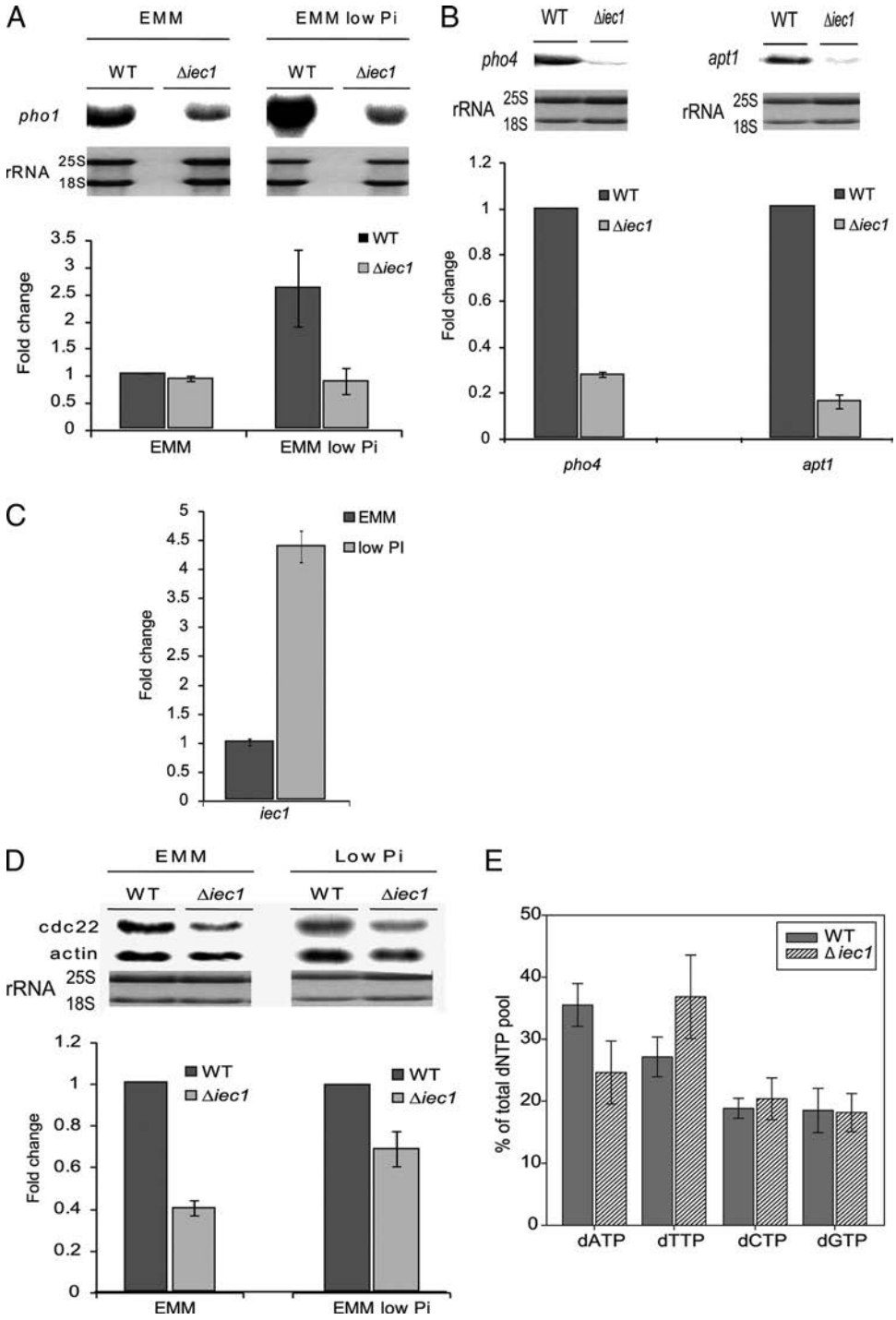

FIG. 4. Iec1 is required for correct *pho1*, *pho4*, *apt1*, and *cdc22* expression. (A) (Top) Northern analysis of *pho1* transcript levels in control (WT; SA001) and Δ*iec1* (CH003) cells. The cells were grown in minimal and low-phosphate minimal media, and *pho1* transcript levels were assayed. (Bottom) Quantification of *pho1* transcript levels by PCR following reverse transcription. The values were normalized to actin and expressed as fold change in expression relative to the control (WT). The error bars represent the standard errors of two independent experiments. (B) Northern analysis of *pho4* and *apt1* transcript levels in control (SA001) and Δ*iec1* (CH003) cells. The cells were grown in low-phosphate minimal or low-phosphate rich medium, and *pho4* and *apt1* transcript levels were quantified. Below is a graphic representation of the values normalized to 25S rRNA from the blots above and expressed as fold change relative to the control (WT). The error bars represent the standard errors of two independent experiments. No change in the expression level of these genes was observed when cells were grown in minimal medium containing normal levels of phosphate. (C) The expression of *iec1* in WT cells grown in minimal medium (EMM) and low-phosphate minimal medium (low Pi) was quantified by PCR following reverse transcription of RNA. The results were normalized to actin and expressed as fold change relative to WT expression in EMM. The error bars represent the standard deviations of two independent experiments. (D) Northern analysis of *cdc22* expression levels in control (SA001) and Δ*iec1* (CH003) cells. The cells were grown in minimal or low-phosphate minimal medium, and *cdc22* transcript levels were quantified. Below is a graphic representation of the values normalized to actin and expressed as fold change relative to the control (WT). The error bars represent the standard errors of two independent experiments. (E) dNTP levels were assayed in control (SA001) and Δ*iec1* (CH003) cells grown in EMM as described in Materials and Methods and expressed as a percentage of the total nucleotide pool. The error bars represent the standard errors of three independent experiments.

A

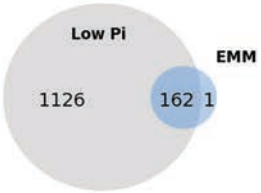

B

> 1.5-fold enrichment	Gene Ontology Categories	Number of genes in overlap	Number of genes in category	Overlap *P*-values
INO80 Targets (163 genes)	GO:0005886 plasma membrane	25	193	2.62E-07
	GO:0003700 transcription factor activity	15	83	1.42E-05
	GO:0005215 transporter activity	25	292	1.21E-03
	GO:0065007 biological regulation	50	953	1.52E-02
	GO:0006811 ion transport	13	113	2.68E-02
New INO80 targets in Low Pi (1126 genes)	GO:0033554 cellular response to stress	174	629	4.74E-02
	GO:0044106 cellular amine metabolic process	62	183	8.45E-02

C

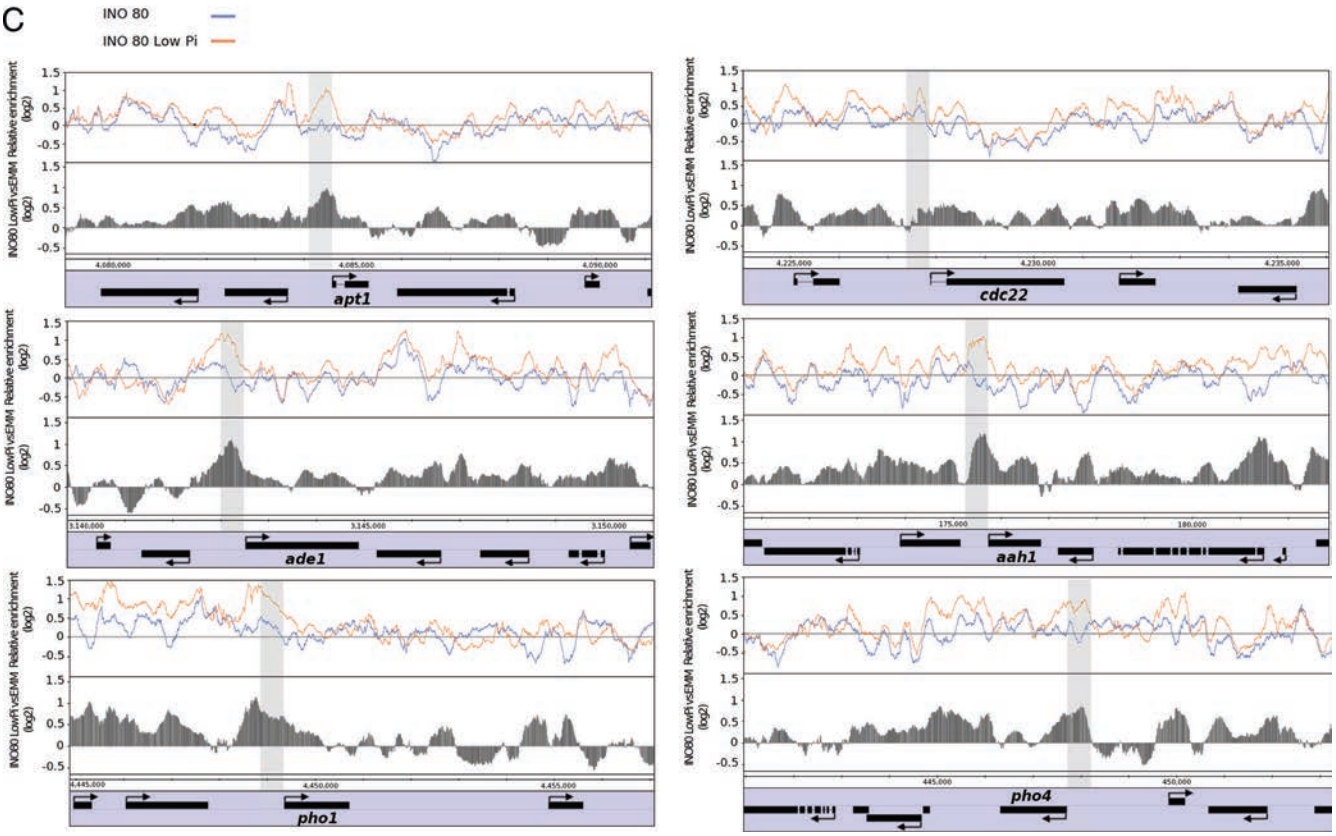

FIG. 5. Ino80 is recruited to the *apt1*, *cdc22*, *ade1*, *aah1*, *pho1*, and *pho4* promoter regions upon phosphate starvation. (A) Venn diagram illustrating the number of promoter regions showing significant Ino80 binding in EMM and low-phosphate EMM. (B) Results of gene ontology analysis of Ino80 target genes. The most significant gene ontology categories, the number of genes in overlap, the number of genes in each category, and the *P* values indicating the significance of the overlap are shown. (C) High-resolution tiling arrays showing the enrichment of Ino80-FLAG in cells growing in low-phosphate EMM compared to normal EMM for the *apt1*, *cdc22*, *ade1*, *aah1*, *pho1*, and *pho4* genes.

involved in phosphate and adenine metabolism upon phosphate starvation, leading to transcription, and that Iec1 is required for efficient binding of the Ino80 complex at its target genes.

Iec1 mediates nucleosome depletion over target genes. We explored whether Iec1 mediates nucleosome remodeling at target genes to facilitate transcription. We tested this by performing ChIP of histone H3, which reflects nucleosome occupancy, over the promoter regions and gene bodies of the Iec1 target genes, *pho1*, *pho4*, *apt1*, and *aah1*, in control and *iec1* deletion strains grown in low-phosphate EMM. We found that in the absence of Iec1, histone H3 occupancy increased at each locus tested. This occurred not only in the upstream region of the genes, but also within the gene bodies themselves (Fig. 8A to D). Interestingly, Iec1 binding, histone occupancy, and the impact of *iec1* deletion on histone occupancy are broadly distributed in the same way over these target genes (compare Fig. 7 and 8). Deletion of Arp8, another component of the Ino80 complex, led to a similar increase in histone density over these genes (data not shown). These *in vivo* data are consistent with the *in vitro* activity of Ino80 that rendered chromatin more accessible (Fig. 1B) and indicate that the presence of Ino80, mediated by Iec1, results in an overall reduction of nucleosomes over target loci.

DISCUSSION

The relationship between fission yeast Iec1-Ino80 and higher-eukaryote YY1-Ino80 complexes. In this study, we found that the fission yeast Ino80 complex is highly conserved through evolution (Table 4). *S. pombe* Ino80 interacts with Iec1, which contains zinc finger motifs similar to those found in YY1, an

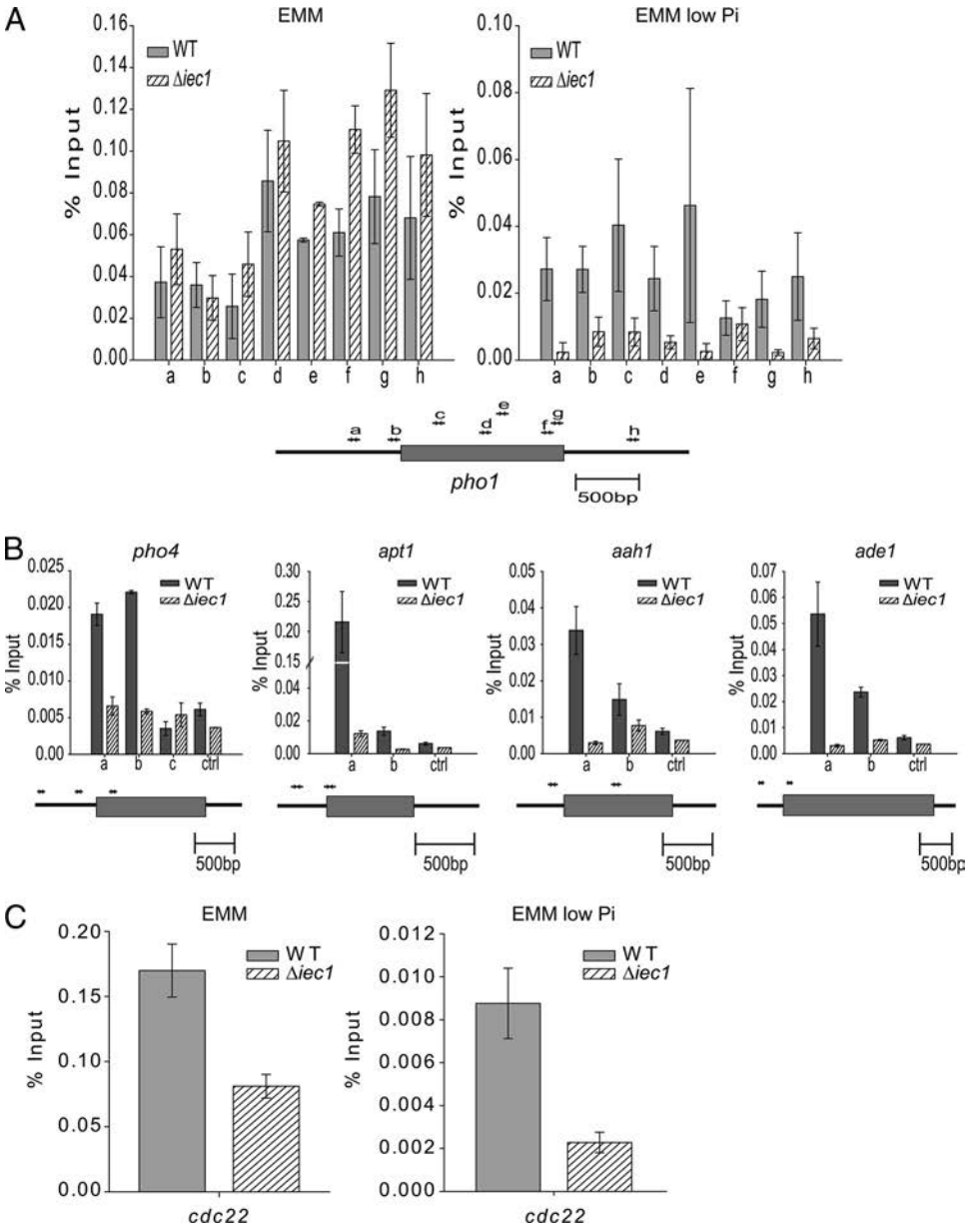

FIG. 6. Iec1 mediates binding of Ino80 to target genes. Ino80 occupancy of Ino80p in control (WT; SA001) and Δ*iec1* (CH003) strains was determined by ChIP at the *pho1* locus (A) and at the *pho4*, *apt1*, *aah1* and *ade1* loci (B) in low-phosphate media. Schematic representations of the loci show the localization of the primer pairs used for quantitative PCR indicated by horizontal arrows. The control locus (ctrl) is 800 bp upstream of the *ade10* open reading frame. (C) Ino80 occupancy of Ino80p in control (SA001) and Δ*iec1* (CH003) strains was determined at a site 800 bp upstream of the *cdc22* ORF in minimal and low-phosphate media. The error bars represent the standard errors of two independent experiments. Gray bars, control strain; hatched bars, Δ*iec1* strain.

Ino80 complex component of higher eukaryotes (10, 41, 82). In budding yeast, there is no clear Iec1 or YY1 homologue. We identified an Iec1-Ino80 core complex that is similar to the *Drosophila* and mammalian YY1/PHO-Ino80 core complexes (Table 4) (10, 41, 82). We tested whether human YY1 can complement Iec1 in its roles in replication stress (HU), temperature stress, and growth without adenine and in low phosphate and found that human YY1 cannot substitute for Iec1 under these conditions, with the exception that it ameliorated the "pink-pigment" phenotype when grown in low phosphate (data not shown). YY1 binds to specific sequence motifs but has recently been shown to also bind structured DNA (four-way junction DNA) in a sequence-independent manner (82). We found no evidence that Iec1 binds specific sequence elements, since it was broadly distributed over target genes (Fig. 7). Its binding seemed to reflect nucleosome density and was consistent with its impact on nucleosome occupancy. It is tempting to speculate that Iec1 may also recognize a specific DNA structure, e.g., the DNA crossovers at the entry-exit sites of the DNA around nucleosomes.

YY1, Ino80, and the YY1-associated Ino80 complex have previously been shown to play roles in the DNA damage re-

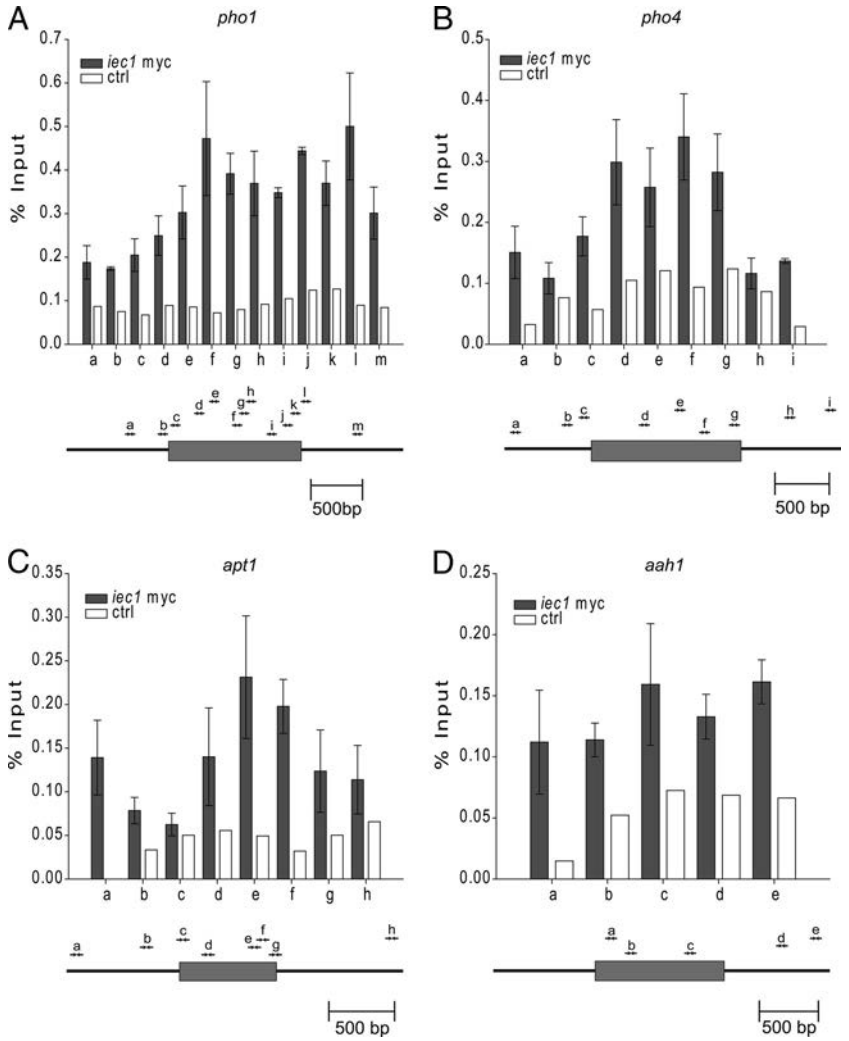

FIG. 7. Iec1 is recruited to genes involved in nucleotide metabolism. ChIP of a MYC-tagged Iec1p strain (CH016) grown in low-phosphate EMM was performed at the *pho1*, *pho4*, *apt1*, and *aah1* loci. The results were normalized to no-antibody control and expressed as a percentage of the input. Anti-MYC ChIP of a nontagged strain was plotted to show background enrichment (ctrl). The error bars represent the standard errors of two independent experiments. Black bars, 13MYC Iec1 strain; white bars, control strain. Below each diagram is a schematic representation of the locus with the localization of the primer pairs used for quantitative PCR indicated by horizontal arrows.

sponse, and our results suggest that this is also the case for the fission yeast Iec1-Ino80 complex (Fig. 2B to D) (1, 65, 82). More recently, the Ino80 complex in budding yeast has been shown to be recruited directly to replication forks (57, 69, 80). It is not known if the mammalian YY1-Ino80 complex has a role in DNA replication. However, our results suggest a role for the Iec1-Ino80 complex in replication, given the sensitivity of Iec1 and Ino80 mutants to the drug HU (Fig. 2B to D).

While Iec1 is required for Ino80 binding, the distributions of Ino80 and Iec1 do not completely mirror each other at target loci. We cannot exclude the possibility that this is the result of epitope exclusion of Iec1 in, for example, the promoter regions of genes. Another explanation could be that not all chromatin-bound Iec1 is in complex with Ino80, but binding of Iec1 to chromatin may be required to load Ino80 onto chromatin. It is possible that Iec1 recognizes a specific histone modification that is upregulated upon phosphate starvation or some other change in chromatin structure. In this respect, it is interesting that *iec1* mRNA is upregulated severalfold upon phosphate starvation (Fig. 4C), indicating that it is part of a concerted stress response involving Ino80.

One question that arises from these results is why Iec1 is present in the fission yeast but not in the budding yeast Ino80 complex. A major difference between budding yeast and fission yeast is the organization of their chromatin structures. Budding yeast exhibits very little higher-order chromatin, whereas fission yeast has extensive heterochromatic domains regulated by the RNA interference machinery, homologues of heterochromatin protein 1, and histone H3 lysine 9 methylation, all of which are absent in budding yeast. Therefore, we might speculate that fission yeast, like higher eukaryotes, requires the presence of a module for Ino80 to guide it through this more complex higher-order chromatin structure.

Interestingly, whereas the single deletions of the Ino80 complex subunit gene *iec1* or *ies2* resulted in loss of viability in low-phosphate medium, the mutant with a double deletion of

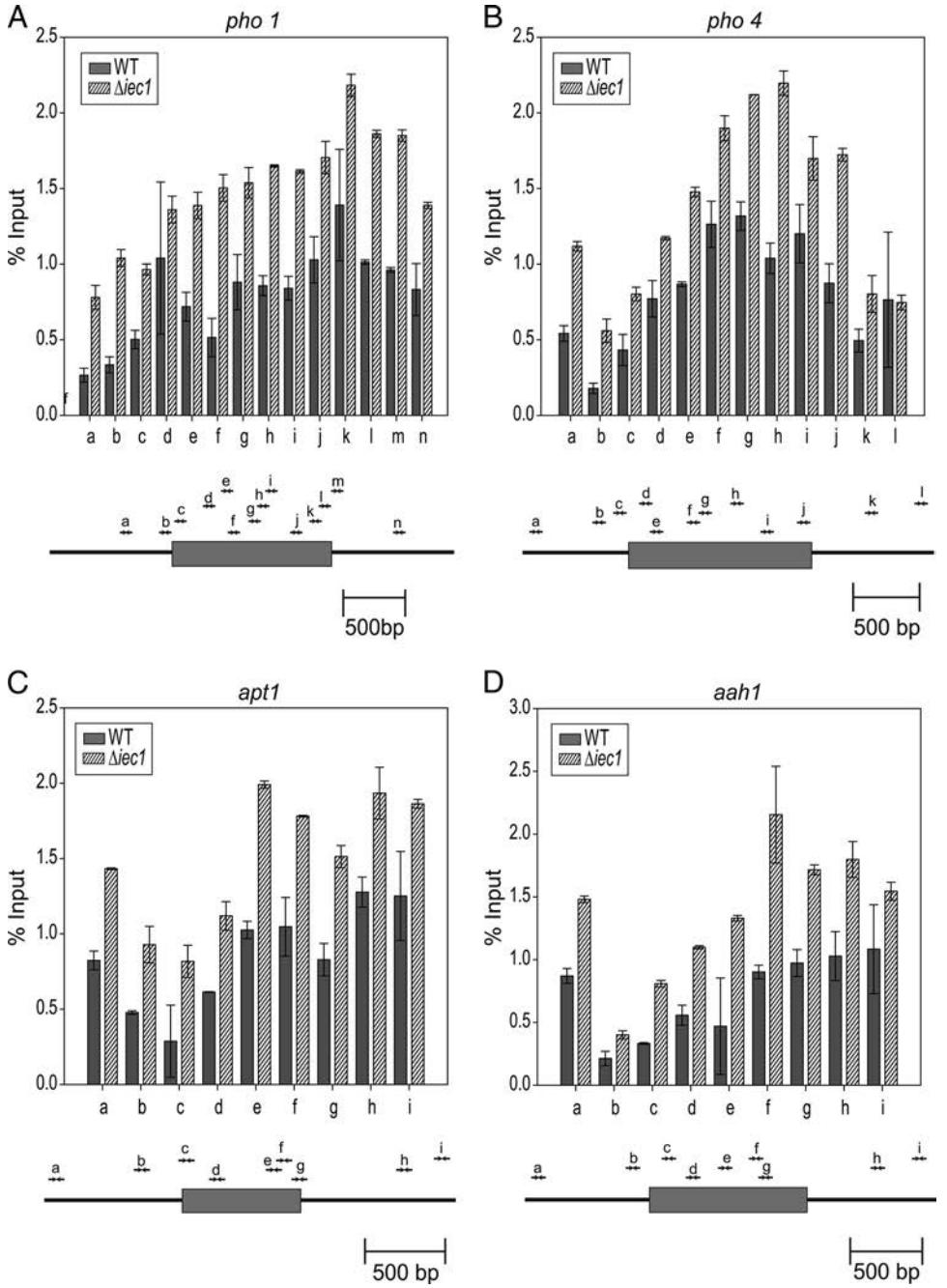

FIG. 8. Iec1 mediates nucleosome eviction at promoters and in the bodies of target genes. (A to D) Chromatin immunoprecipitation of histone H3 in control (WT; SA001) and Δ*iec1* (CH003) strains grown in low-phosphate EMM was performed at the *pho1*, *pho4*, *apt1*, and *aah1* loci. The error bars represent the standard errors of two independent experiments. Black bars, control; hatched bars, Δ*iec1*. The diagrams show a schematic representation of each locus with the localization of primer pairs used for quantitative PCR indicated by horizontal arrows.

iec1 and *ies2* was almost as viable as the control cells under this condition. Null alleles in two subunits of the same complex usually show a nonadditive phenotype. One possible explanation is that the suppression phenotype observed in the double mutants is the result of partial complexes that are formed in single mutants and are inhibitory to cell function. An alternative explanation is that Iec1 is in a distinct complex (or functions in isolation) whose function is antagonized by an Ies2-containing complex. This explanation may be more attractive, given that the alleles are nulls, not partial loss-of-function alleles. Therefore, different Ino80 complex components may program opposing functions of Ino80.

Iec1-Ino80 regulates histone density over target genes. Earlier work showed that Ino80 mediates nucleosome eviction at DNA double-strand breaks and that this eviction is important for subsequent DNA repair (52, 56, 74–76). Ino80 has been shown to cooperate with SWI/SNF in nucleosome remodeling at the INO1 and PHO5 promoters in budding yeast (5, 23).

However, little is known about how Ino80 remodels chromatin for gene expression. Our results suggest that fission yeast Iec1 and Ino80 cooperate in gene regulation by mediating gene-specific chromatin remodeling. We showed for the first time that Ino80 is involved in the loss of nucleosome density within the promoter regions and bodies of genes (Fig. 8). It is tempting to speculate that Ino80-mediated nucleosome loss over genes underlies the role of Ino80 in transcription, e.g., by facilitating preinitiation complex assembly, RNA polymerase promoter escape, or transcription elongation.

A role for Iec1 in the cross talk between phosphate and nucleotide metabolism. We found that the Δ*iec1* mutants and mutants of other components of the Ino80 complex are sensitive to low levels of phosphate, and under phosphate starvation, the Δ*iec1* mutants appear to activate the *de novo* synthesis pathway of adenine metabolism (Fig. 3B). This was confirmed by the finding that Δ*iec1* and Ino80 complex mutants displayed an altered phenotype when grown on low-adenine medium (Fig. 3B). The mutants also displayed defects in sporulation when grown under either phosphate- or adenine-limiting conditions (Fig. 3D). Taken together, these findings suggest that there is cross talk between phosphate and adenine metabolic pathways. The requirement for this cross talk within the cell can be explained by the fact that nucleotides are abundant biomolecules and their synthesis is associated with significant phosphate consumption. It therefore seems imperative for cells to evolve regulatory mechanisms to coordinate phosphate utilization and nucleotide synthesis. For example, in budding yeast, the Pho2p transcription factor is required for purine de novo biosynthesis and phosphate utilization pathways (14, 58). Ado1, which encodes an adenosine kinase, negatively regulates PHO5 expression, and the deletion of adenylate kinase (Adk1p) strongly induces the expression of the PHO and ADE genes involved in phosphate utilization and AMP de novo biosynthesis, respectively (27, 33). Our results suggest that a functional Iec1-Ino80 complex is required to ensure this coordinated cross talk within the cell.

We showed that Iec1 regulates the transcription of genes involved in phosphate and adenine metabolism and the recruitment of the Ino80 complex to these genes upon phosphate starvation (Fig. 4C, 5C, and 6C). This indicates that the Iec1-Ino80 complex is involved in transcriptional regulation. Ino80 has also been shown by several laboratories to have a direct role in repair in budding yeast (52, 56, 74–76). Therefore, we do not believe that the impaired DNA damage response in cells with an impaired Ino80 complex is simply due to altered gene expression in *S. pombe*. Since phosphate and nucleotides are essential constituents of many essential biomolecules, their misregulation may influence cellular processes, such as replication and repair. We propose that by regulating phosphate and nucleotide metabolism, the Ino80 complex integrates its role in transcription with its roles in replication and repair. This ensures an integrated response when exposed to cellular stress.

ACKNOWLEDGMENTS

We thank Jacob Dalgaard for yeast strains, initial guidance in fission yeast techniques, and discussion; Robin Allshire and Susan Forsburg for yeast strains; and Jürgen Kohli and Yang Shi for plasmids. We thank one anonymous referee for help with the explanation of the *iec1 ies2* double-deletion phenotype; Colin Goding for providing bench space to S.A.; and Peter Fraser, Cameron Osbourne, and Jacqueline Mermoud for comments that improved the manuscript.

This work was supported by a BBSRC studentship (to C.J.H.), a Marie Curie Cancer Care studentship (to S.A.), and a BBSRC grant to the P.D.V.-W. laboratory (BB/F020236/1). Work in the P.D.V.-W. and K.E. laboratories was supported by the EU through the Epigenome Network of Excellence. Work in the K.E. laboratory was also supported by the Swedish Cancer Fund and the Swedish Research Council. Work in the C.K.M. laboratory was supported by grant no. 49557LS from the U.S. Army Research Office. S.E. is supported by a Wellcome Trust Career Development Award.

REFERENCES

1. **Affar, E. B., F. Gay, Y. Shi, H. Liu, M. Huarte, S. Wu, T. Collins, E. Li, and Y. Shi.** 2006. Essential dosage-dependent functions of the transcription factor yin yang 1 in late embryonic development and cell cycle progression. Mol. Cell. Biol. **26:**3565–3581.
2. **Altschul, S. F., and E. V. Koonin.** 1998. Iterated profile searches with PSI-BLAST—a tool for discovery in protein databases. Trends Biochem. Sci. **23:**444–447.
3. **Bähler, J., J. Q. Wu, M. S. Longtine, N. G. Shah, A. McKenzie, A. B. Steever, A. Wach, P. Philippsen, and J. R. Pringle.** 1998. Heterologous modules for efficient and versatile PCR-based gene targeting in *Schizosaccharomyces pombe*. Yeast **14:**943–951.
4. **Bao, Y., and X. Shen.** 2007. INO80 subfamily of chromatin remodeling complexes. Mutat. Res. **618:**18–29.
5. **Barbaric, S., T. Luckenbach, A. Schmid, D. Blaschke, W. Horz, and P. Korber.** 2007. Redundancy of chromatin remodeling pathways for the induction of the yeast PHO5 promoter in vivo. J. Biol. Chem. **282:**27610–27621.
6. **Becker, P. B., and W. Horz.** 2002. ATP-dependent nucleosome remodeling. Annu. Rev. Biochem. **71:**247–273.
7. **Berger, S. L.** 2007. The complex language of chromatin regulation during transcription. Nature **447:**407–412.
8. **Bianchi, V., E. Pontis, and P. Reichard.** 1986. Changes of deoxyribonucleoside triphosphate pools induced by hydroxyurea and their relation to DNA synthesis. J. Biol. Chem. **261:**16037–16042.
9. **Brown, J. L., D. Mucci, M. Whiteley, M.-L. Dirksen, and J. A. Kassis.** 1998. The Drosophila Polycomb group gene pleiohomeotic encodes a DNA binding protein with homology to the transcription factor YY1. Mol. Cell **1:**1057–1064.
10. **Cai, Y., J. Jin, T. Yao, A. J. Gottschalk, S. K. Swanson, S. Wu, Y. Shi, M. P. Washburn, L. Florens, R. C. Conaway, and J. W. Conaway.** 2007. YY1 functions with INO80 to activate transcription. Nat. Struct. Mol. Biol. **14:**872–874.
11. **Cairns, B. R., N. L. Henry, and R. D. Kornberg.** 1996. TFG/TAF30/ANC1, a component of the yeast SWI/SNF complex that is similar to the leukemogenic proteins ENL and AF-9. Mol. Cell. Biol. **16:**3308–3316.
12. **Chabes, A., B. Georgieva, V. Domkin, X. Zhao, R. Rothstein, and L. Thelander.** 2003. Survival of DNA damage in yeast directly depends on increased dNTP levels allowed by relaxed feedback inhibition of ribonucleotide reductase. Cell **112:**391–401.
13. **Choudhary, P., and P. Varga-Weisz.** 2007. ATP-dependent chromatin remodelling: action and reaction. Subcell. Biochem. **41:**29–43.
14. **Daignan-Fornier, B., and G. R. Fink.** 1992. Coregulation of purine and histidine biosynthesis by the transcriptional activators BAS1 and BAS2. Proc. Natl. Acad. Sci. U. S. A. **89:**6746–6750.
15. **Donohoe, M. E., X. Zhang, L. McGinnis, J. Biggers, E. Li, and Y. Shi.** 1999. Targeted disruption of mouse Yin Yang 1 transcription factor results in peri-implantation lethality. Mol. Cell. Biol. **19:**7237–7244.
16. **Downs, J. A., S. Allard, O. Jobin-Robitaille, A. Javaheri, A. Auger, N. Bouchard, S. J. Kron, S. P. Jackson, and J. Cote.** 2004. Binding of chromatin-modifying activities to phosphorylated histone H2A at DNA damage sites. Mol. Cell **16:**979–990.
17. **Durand-Dubief, M., and K. Ekwall.** 2009. Chromatin immunoprecipitation using microarrays. Methods Mol. Biol. **529:**279–295.
18. **Ebbert, R., A. Birkmann, and H. J. Schuller.** 1999. The product of the SNF2/SWI2 paralogue INO80 of Saccharomyces cerevisiae required for efficient expression of various yeast structural genes is part of a high-molecular-weight protein complex. Mol. Microbiol. **32:**741–751.
19. **Elble, R.** 1992. A simple and efficient procedure for transformation of yeasts. Biotechniques **13:**18–20.
20. **Elledge, S. J., Z. Zhou, and J. B. Allen.** 1992. Ribonucleotide reductase: regulation, regulation, regulation. Trends Biochem. Sci. **17:**119–123.
21. **Fernandez Sarabia, M. J., C. McInerny, P. Harris, and P. Fantes.** 1993. The cell cycle genes cdc22+ and suc22+ of the fission yeast Schizosaccharomyces pombe encode the large and small subunits of ribonucleotide reductase. Mol. Gen. Genet. **238:**241–251.
22. **Finn, R. D., J. Tate, J. Mistry, P. C. Coggill, S. J. Sammut, H.-R. Hotz, G.**

Ceric, K. Forslund, S. R. Eddy, E. L. L. Sonnhammer, and A. Bateman. 2008. The Pfam protein families database. Nucleic Acids Res. **36:**D281–D288.
23. **Ford, J., O. Odeyale, A. Eskandar, N. Kouba, and C. H. Shen.** 2007. A SWI/SNF- and INO80-dependent nucleosome movement at the INO1 promoter. Biochem. Biophys. Res. Commun. **361:**974–979.
24. **Fritsch, O., G. Benvenuto, C. Bowler, J. Molinier, and B. Hohn.** 2004. The INO80 protein controls homologous recombination in Arabidopsis thaliana. Mol. Cell **16:**479–485.
25. **Gallant, P.** 2007. Control of transcription by Pontin and Reptin. Trends Cell Biol. **17:**187–192.
26. **Gangaraju, V. K., and B. Bartholomew.** 2007. Mechanisms of ATP dependent chromatin remodeling. Mut. Res. **618:**3–17.
27. **Gauthier, S., F. Coulpier, L. Jourdren, M. Merle, S. Beck, M. Konrad, B. Daignan-Fornier, and B. Pinson.** 2008. Co-regulation of yeast purine and phosphate pathways in response to adenylic nucleotide variations. Mol. Microbiol. **68:**1583–1594.
28. **Grewal, S. I., and S. Jia.** 2007. Heterochromatin revisited. Nat. Rev. Genet. **8:**35–46.
29. **Grimm, C., J. Kohli, J. Murray, and K. Maundrell.** 1988. Genetic engineering in Schizosaccharomyces pombe: a system for gene disruption and replacement using the ura4 gene as a selectable marker. Mol. Gen. Genet. **215:**81–86.
30. **Henry, N. L., A. M. Campbell, W. J. Feaver, D. Poon, P. A. Weil, and R. D. Kornberg.** 1994. TFIIF-TAF-RNA polymerase II connection. Genes Dev. **8:**2868–2878.
31. **Henry, N. L., M. H. Sayre, and R. D. Kornberg.** 1992. Purification and characterization of yeast RNA polymerase II general initiation factor g. J. Biol. Chem. **267:**23388–23392.
32. **Hentges, P., B. Van Driessche, L. Tafforeau, J. Vandenhaute, and A. M. Carr.** 2005. Three novel antibiotic marker cassettes for gene disruption and marker switching in *Schizosaccharomyces pombe*. Yeast **22:**1013–1019.
33. **Huang, S., and E. K. O'Shea.** 2005. A systematic high-throughput screen of a yeast deletion collection for mutants defective in PHO5 regulation. Genetics **169:**1859–1871.
34. **Ikura, T., V. V. Ogryzko, M. Grigoriev, R. Groisman, J. Wang, M. Horikoshi, R. Scully, J. Qin, and Y. Nakatani.** 2000. Involvement of the TIP60 histone acetylase complex in DNA repair and apoptosis. Cell **102:**463–473.
35. **Jenuwein, T., and C. D. Allis.** 2001. Translating the histone code. Science **293:**1074–1080.
36. **Jin, J., Y. Cai, T. Yao, A. J. Gottschalk, L. Florens, S. K. Swanson, J. L. Gutierrez, M. K. Coleman, J. L. Workman, A. Mushegian, M. P. Washburn, R. C. Conaway, and J. W. Conaway.** 2005. A mammalian chromatin remodeling complex with similarities to the yeast INO80 complex. J. Biol. Chem. **280:**41207–41212.
37. **Johnsson, A., M. Durand-Dubief, Y. Xue-Franzen, M. Ronnerblad, K. Ekwall, and A. Wright.** 2009. HAT-HDAC interplay modulates global histone H3K14 acetylation in gene-coding regions during stress. EMBO Rep. **10:**1009–1014.
38. **Jónsson, Z. O., S. Jha, J. A. Wohlschlegel, and A. Dutta.** 2004. Rvb1p/Rvb2p recruit Arp5p and assemble a functional Ino80 chromatin remodeling complex. Mol. Cell **16:**465–477.
39. **Kawashima, S., H. Ogiwara, S. Tada, M. Harata, U. Wintersberger, T. Enomoto, and M. Seki.** 2007. The INO80 complex is required for damage-induced recombination. Biochem. Biophys. Res. Commun. **355:**835–841.
40. **Kimura, M., and A. Ishihama.** 2004. Tfg3, a subunit of the general transcription factor TFIIF in Schizosaccharomyces pombe, functions under stress conditions. Nucleic Acids Res. **32:**6706–6715.
41. **Klymenko, T., B. Papp, W. Fischle, T. Kocher, M. Schelder, C. Fritsch, B. Wild, M. Wilm, and J. Muller.** 2006. A Polycomb group protein complex with sequence-specific DNA-binding and selective methyl-lysine-binding activities. Genes Dev. **20:**1110–1122.
42. **Kobor, M. S., S. Venkatasubrahmanyam, M. D. Meneghini, J. W. Gin, J. L. Jennings, A. J. Link, H. D. Madhani, and J. Rine.** 2004. A protein complex containing the conserved Swi2/Snf2-related ATPase Swr1p deposits histone variant H2A.Z into euchromatin. PLoS Biol. **2:**e131.
43. **Krogan, N. J., M.-C. Keogh, N. Datta, C. Sawa, O. W. Ryan, H. Ding, R. A. Haw, J. Pootoolal, A. Tong, V. Canadien, D. P. Richards, X. Wu, A. Emili, T. R. Hughes, S. Buratowski, and J. F. Greenblatt.** 2003. A Snf2 Family ATPase complex required for recruitment of the histone H2A variant Htz1. Mol. Cell **12:**1565–1576.
44. **Kurdistani, S. K., D. Robyr, S. Tavazoie, and M. Grunstein.** 2002. Genome-wide binding map of the histone deacetylase Rpd3 in yeast. Nat. Genet. **31:**248–254.
45. **Li, B., M. Carey, and J. L. Workman.** 2007. The role of chromatin during transcription. Cell **128:**707–719.
46. **Livak, K. J., and T. D. Schmittgen.** 2001. Analysis of relative gene expression data using real-time quantitative PCR and the 2(-Delta Delta C(T)) method. Methods **25:**402–408.
47. **Luger, K., T. J. Rechsteiner, and T. J. Richmond.** 1999. Expression and purification of recombinant histones and nucleosome reconstitution. Methods Mol. Biol. **119:**1–16.
48. **Mathews, C. K., and L. J. Wheeler.** 2009. Measuring DNA precursor pools in mitochondria, p. 371–381. *In* J. A. Stuart (ed.), Mitochondrial DNA: methods and protocols, 2nd ed. Methods in molecular biology series. Humana Press, Totowa, NJ.
49. **Maundrell, K., P. Nurse, F. Schönholzer, and M. E. Schweingruber.** 1985. Cloning and characterization of two genes restoring acid phosphatase activity in pho1− mutants of Schizosaccharomyces pombe. Gene **39:**223–230.
50. **Mizuguchi, G., X. Shen, J. Landry, W.-H. Wu, S. Sen, and C. Wu.** 2004. ATP-driven exchange of histone H2AZ variant catalyzed by SWR1 chromatin remodeling complex. Science **303:**343–348.
51. **Moreno, S., A. Klar, and P. Nurse.** 1991. Molecular genetic analysis of fission yeast *Schizosaccharomyces pombe*. Methods Enzymol. **194:**795–823.
52. **Morrison, A. J., J. Highland, N. J. Krogan, A. Arbel-Eden, J. F. Greenblatt, J. E. Haber, and X. Shen.** 2004. INO80 and [gamma]-H2AX interaction links ATP-dependent chromatin remodeling to DNA damage repair. Cell **119:**767–775.
53. **Nabatiyan, A., D. Szuts, and T. Krude.** 2006. Induction of CAF-1 expression in response to DNA strand breaks in quiescent human cells. Mol. Cell. Biol. **26:**1839–1849.
54. **Narlikar, G. J., H.-Y. Fan, and R. E. Kingston.** 2002. Cooperation between complexes that regulate chromatin structure and transcription. Cell **108:**475–487.
55. **Nordlund, P., and P. Reichard.** 2006. Ribonucleotide reductases. Annu. Rev. Biochem. **75:**681–706.
56. **Papamichos-Chronakis, M., J. E. Krebs, and C. L. Peterson.** 2006. Interplay between Ino80 and Swr1 chromatin remodeling enzymes regulates cell cycle checkpoint adaptation in response to DNA damage. Genes Dev. **20:**2437–2449.
57. **Papamichos-Chronakis, M., and C. L. Peterson.** 2008. The Ino80 chromatin-remodeling enzyme regulates replisome function and stability. Nat. Struct. Mol. Biol. **15:**338–345.
58. **Rebora, K., C. Desmoucelles, F. Borne, B. Pinson, and B. Daignan-Fornier.** 2001. Yeast AMP pathway genes respond to adenine through regulated synthesis of a metabolic intermediate. Mol. Cell. Biol. **21:**7901–7912.
59. **Robyr, D., and M. Grunstein.** 2003. Genomewide histone acetylation microarrays. Methods **31:**83–89.
60. **Schweingruber, M. E., R. Fluri, K. Maundrell, A. M. Schweingruber, and E. Dumermuth.** 1986. Identification and characterization of thiamin repressible acid phosphatase in yeast. J. Biol. Chem. **261:**15877–15882.
61. **Schweingruber, M. E., E. Edenharter, A. Zurlinden, and K. M. Stockmaier.** 1992. Regulation of pho1-encoded acid phosphatase of Schizosaccharomyces pombe by adenine and phosphate. Curr. Genet. **22:**289–292.
62. **Schweingruber M. E., and A. Schweingruber.** 1981. Modulation of a cell surface glycoprotein in yeast: acid phosphatase. Differentiation **19:**68–70.
63. **Shen, X., R. Ranallo, E. Choi, and C. Wu.** 2003. Involvement of actin-related proteins in ATP-dependent chromatin remodeling. Mol. Cell **12:**147–155.
64. **Shen, X., H. Xiao, R. Ranallo, W.-H. Wu, and C. Wu.** 2003. Modulation of ATP-dependent chromatin-remodeling complexes by inositol polyphosphates. Science **299:**112–114.
65. **Shen, X., G. Mizuguchi, A. Hamiche, and C. Wu.** 2000. A chromatin remodelling complex involved in transcription and DNA processing. Nature **406:**541–544.
66. **Sherman, P. A., and J. A. Fyfe.** 1989. Enzymatic assay for deoxyribonucleoside triphosphates using synthetic oligonucleotides as template primers. Anal. Biochem. **180:**222–226.
67. **Shevchenko, A., A. Roguev, D. Schaft, L. Buchanan, B. Habermann, C. Sakalar, H. Thomas, N. J. Krogan, and A. F. Stewart.** 2008. Chromatin central: towards the comparative proteome by accurate mapping of the yeast proteomic environment. Genome Biol. **9:**R167.
68. **Shi, Y., J.-S. Lee, and K. M. Galvin.** 1997. Everything you have ever wanted to know about Yin Yang 1. Biochim. Biophys. Acta **1332:**F49–F66.
69. **Shimada, K., Y. Oma, T. Schleker, K. Kugou, K. Ohta, M. Harata, and S. M. Gasser.** 2008. Ino80 chromatin remodeling complex promotes recovery of stalled replication forks. Curr. Biol. **18:**566–575.
70. **Sinha, R. P., and D. P. Hader.** 2002. UV-induced DNA damage and repair: a review. Photochem. Photobiol. Sci. **1:**225–236.
71. **Steger, D. J., E. S. Haswell, A. L. Miller, S. R. Wente, and E. K. O'Shea.** 2003. Regulation of chromatin remodeling by inositol polyphosphates. Science **299:**114–116.
72. **Stepchenkova, E., S. Kozmin, V. Alenin, and Y. Pavlov.** 2005. Genome-wide screening for genes whose deletions confer sensitivity to mutagenic purine base analogs in yeast. BMC Genet. **6:**31.
73. **Tsukiyama, T., J. Palmer, C. C. Landel, J. Shiloach, and C. Wu.** 1999. Characterization of the Imitation Switch subfamily of ATP-dependent chromatin-remodeling factors in Saccharomyces cerevisiae. Genes Dev. **13:**686–697.
74. **Tsukuda, T., A. B. Fleming, J. A. Nickoloff, and M. A. Osley.** 2005. Chromatin remodelling at a DNA double-strand break site in Saccharomyces cerevisiae. Nature **438:**379–383.
75. **van Attikum, H., O. Fritsch, and S. M. Gasser.** 2007. Distinct roles for SWR1 and INO80 chromatin remodeling complexes at chromosomal double-strand breaks. EMBO J. **26:**4113–4125.
76. **van Attikum, H., O. Fritsch, B. Hohn, and S. M. Gasser.** 2004. Recruitment of the INO80 complex by H2A phosphorylation links ATP-dependent chromatin remodeling with DNA double-strand break repair. Cell **119:**777–788.

77. **van Attikum, H., and S. M. Gasser.** 2005. ATP-dependent chromatin remodeling and DNA double-strand break repair. Cell Cycle **4:**1011–1014.
78. **Van Driessche, B., L. Tafforeau, P. Hentges, A. M. Carr, and J. Vandenhaute.** 2005. Additional vectors for PCR-based gene tagging in Saccharomyces cerevisiae and Schizosaccharomyces pombe using nourseothricin resistance. Yeast **22:**1061–1068.
79. **Varga-Weisz, P. D., E. J. Bonte, and P. B. Becker.** 1999. Analysis of modulators of chromatin structure in Drosophila. Methods Enzymol. **304:**742–757.
80. **Vincent, J. A., T. J. Kwong, and T. Tsukiyama.** 2008. ATP-dependent chromatin remodeling shapes the DNA replication landscape. Nat. Struct. Mol. Biol. **15:**477–484.
81. **Wood, M. A., S. B. McMahon, and M. D. Cole.** 2000. An ATPase/helicase complex is an essential cofactor for oncogenic transformation by c-Myc. Mol. Cell **5:**321–330.
82. **Wu, S., Y. Shi, P. Mulligan, F. Gay, J. Landry, H. Liu, J. Lu, H. H. Qi, W. Wang, J. A. Nickoloff, C. Wu, and Y. Shi.** 2007. A YY1-INO80 complex regulates genomic stability through homologous recombination-based repair. Nat. Struct. Mol. Biol. **14:**1165–1172.
83. **Xue, Y., S. A. Haas, L. Brino, A. Gusnanto, M. Reimers, D. Talibi, M. Vingron, K. Ekwall, and A. P. Wright.** 2004. A DNA microarray for fission yeast: minimal changes in global gene expression after temperature shift. Yeast **21:**25–39.
84. **Zhou, Z., and S. J. Elledge.** 1993. DUN1 encodes a protein kinase that controls the DNA damage response in yeast. Cell **75:**1119–1127.